POLITECNICO DI TORINO
Repository ISTITUZIONALE

Investigating the composition of the K0(700) state with ±KS0 correlations at the LHC

Original
Investigating the composition of the K0(700) state with ±KS0 correlations at the LHC / Acharya, S., Adamová, D., Aglieri Rinella, G., Aglietta, L., Agnello, M., Agrawal, N., Ahammed, Z., Ahmad, S., Ahn, S.U., Ahuja, I., Akindinov, A., Al-Turany, M., Aleksandrov, D., Alessandro, B., Alfanda, H.M., Alfaro Molina, R., Ali, B., Alici, A., Alizadehvandchali, N., Alkin, A., et al.. - In: PHYSICS LETTERS. SECTION B. - ISSN 0370-2693. - STAMPA. - 856:(2024). [10.1016/j.physletb.2024.138915]

Availability:
This version is available at: 11583/3001071 since: 2025-06-18T08:09:21Z

Publisher:
Elsevier B.V.

Published
DOI:10.1016/j.physletb.2024.138915

Terms of use:

This article is made available under terms and conditions as specified in the corresponding bibliographic description in the repository

Publisher copyright

(Article begins on next page)

28 November 2026

Phys. Lett. B 856 (2024) 138915

Contents lists available at ScienceDirect

Physics Letters B

journal homepage: www.elsevier.com/locate/physletb

Letter

Investigating the composition of the $K_0^*(700)$ state with $\pi^{\pm}K_S^0$ correlations at the LHC

ALICE Collaboration *

ARTICLE INFO

Editor: M. Doser

Dataset link: https://www.hepdata.net/record/ins2739149

ABSTRACT

The first measurements of femtoscopic correlations with the particle pair combinations $\pi^{\pm}K_S^0$ in pp collisions at $\sqrt{s} = 13$ TeV at the Large Hadron Collider (LHC) are reported by the ALICE experiment. Using the femtoscopic approach, it is shown that it is possible to study the elusive $K_0^*(700)$ particle that has been considered a tetraquark candidate for over forty years. Source and final-state interaction parameters are extracted by fitting a model assuming a Gaussian source to the experimentally measured two-particle correlation functions. The final-state interaction in the $\pi^{\pm}K_S^0$ system is modeled through a resonant scattering amplitude, defined in terms of a mass and a coupling parameter, The extracted mass and Breit–Wigner width, derived from the coupling parameter, of the final-state interaction are found to be consistent with previous measurements of the $K_0^*(700)$. The small value and increase of the correlation strength with increasing source size support the hypothesis that the $K_0^*(700)$ is a four-quark state, i.e. a tetraquark state of the form $(q_1, \overline{q_2}, q_3, \overline{q_3})$ in which q_1, q_2 and q_3 indicate the flavor of the valence quarks of the π and K_S^0. This latter trend is also confirmed via a simple geometric model that assumes a tetraquark structure of the $K_0^*(700)$ resonance.

1. Introduction

Femtoscopy with identical charged pions has been a useful tool for many years to experimentally probe the geometry of the space-time structure of the freeze-out probability distribution in high-energy pp and heavy-ion collisions [1]. Identical-kaon femtoscopic measurements have also been carried out to complement the identical pion studies, examples of which are measurements in Au–Au collisions at center-of-mass energy per nucleon pair $\sqrt{s_{\rm NN}} = 200$ GeV at the Relativistic Heavy-Ion Collider by the STAR Collaboration [2] ($K_S^0K_S^0$) and PHENIX Collaboration [3] ($K^{\pm}K^{\pm}$), and for pp collisions at $\sqrt{s} = 5.02$, 7, and 13 TeV and Pb–Pb collisions at $\sqrt{s_{\rm NN}} = 2.76$ TeV at the CERN LHC by the ALICE Collaboration [4–7] ($K_S^0K_S^0$ and $K^{\pm}K^{\pm}$).

In the femtoscopic method, the momentum correlations of pairs of particles when interactions with the other particles in the collision system cease, i.e. during "freeze out" [8], can be utilized to get insight into the strength of the pair interaction, i.e. the final-state interaction (FSI), at low relative momentum. The homogeneity region size, the strength, and even the nature of the FSI at freeze out can be determined by fitting the experimental two-particle correlation function to a model based on the FSI. Results on non-identical kaon femtoscopy with $K_S^0K^{\pm}$ pairs were published by ALICE in pp collisions at $\sqrt{s} = 5.02$, 7, and 13 TeV and Pb–Pb collisions at $\sqrt{s_{\rm NN}} = 2.76$ TeV [7,9,10]. Although the general goals of non-identical kaon femtoscopy studies overlap with those for identical kaon femtoscopy, e.g. to extract information about the space–time geometry of the collision region and determine the pair-wise interaction strength, the latter is different in each case. For the identical kaon cases, in which pair-wise quantum statistical correlations are present, the interactions are the following: $K^{\pm}K^{\pm}$ – Coulomb interaction, and $K_S^0K_S^0$ – strong FSI through the $f_0(980)/a_0(980)$ resonances. For the $K_S^0K^{\pm}$ pairs, there are no quantum statistical correlations and the only interaction present is the strong FSI through the $a_0(980)$ resonance.

$K_S^0K^{\pm}$ femtoscopy should thus be sensitive to the properties of the $a_0(980)$ resonance. It has been suggested in many papers in the literature that the $a_0(980)$ could be a four-quark or tetraquark state [11]. It was first proposed in 1977 that experimentally-observed low-lying mesons, such as the $a_0(980)$ and $K_0^*(700)$, are part of a SU(3) tetraquark nonet using the MIT Bag model [12], which was later followed up with lattice QCD calculations [13]. There have been a number of QCD studies of these mesons that can be categorized as QCD-inspired models, see for example Refs. [11,14–16], and lattice QCD calculations, see for example Refs. [17–19].

Indeed, the results of the ALICE $K_S^0K^{\pm}$ studies mentioned above suggested that the $a_0(980)$ is a tetraquark state. This suggestion is based on comparing the extracted pair-wise interaction strength of $K_S^0K^{\pm}$ between pp and Pb–Pb collisions as well as with the $K_S^0K_S^0$ studies [4,6,7,9,10].

* E-mail address: alice-publications@cern.ch.

https://doi.org/10.1016/j.physletb.2024.138915
Received 6 January 2024; Received in revised form 21 June 2024; Accepted 25 July 2024
Available online 30 July 2024
0370-2693/© 2024 CERN for the benefit of the ALICE Collaboration. Published by Elsevier B.V. Funded by SCOAP³. This is an open access article under the CC BY license (http://creativecommons.org/licenses/by/4.0/).

From a geometric picture, since a tetraquark version of the $a_0(980)$ contains a strange – anti-strange quark pair, a FSI through it should be suppressed for a small system as in pp collisions due to an increased annihilation probability, whereas for a large Pb–Pb collision this suppression should not be present. Thus, a strong FSI would be expected from Pb–Pb collisions and weak FSI from pp collisions, and this is what was observed in experiments. It would also be expected that a strong pair-wise correlation would be seen for $K^0_S K^0_S$ studies since quantum statistics is dominant over FSI effects. This exception is corroborated by experimental findings [4,6,7].

The success of the ALICE $K^0_S K^{\pm}$ studies on the nature of the $a_0(980)$ resonance motivated the first femtoscopic study ever of $\pi^{\pm}K^0_S$ correlations in $\sqrt{s} = 13$ TeV pp collisions. Another resonance that is a tetraquark candidate is the $K^*_0(700)$ that decays with a branching ratio of $\sim 100\%$ into πK pairs [12]. The $K^*_0(700)$ is listed in the Review of Particle Physics [20] as a strange meson with spin 0 and isospin $\frac{1}{2}$, the quark content of the $K^*_0(700)^+$ state being $u\bar{s}$. Its mass is listed as 845 ± 17 MeV/c^2 and it is a very broad resonance with Breit–Wigner width of 468 ± 30 MeV/c^2. The mass of the $K^*_0(700)$ is above the $\pi^{\pm}K^0_S$ threshold, that is of about 637.18 MeV/c^2, and its width is seen to encompass this threshold and below. The tetraquark version of the $K^*_0(700)^+$ would have quark content $u\bar{s}d\bar{d}$ and would decay by direct quark transfer into a π^+K^0 pair [12]. Thus by measuring $\pi^{\pm}K^0_S$ correlations it should be possible to study the quark nature of the $K^*_0(700)$ using similar methods as mentioned above for the $a_0(980)$ studies, i.e. measuring the strength of the FSI, assuming that the $\pi^{\pm}K^0_S$ FSI goes solely through the $K^*_0(700)$. This scenario will be studied by extracting the mass and width parameters of the FSI and comparing them with previous measurements of the $K^*_0(700)$ [21]. In the present Letter, a study of femtoscopic correlations with the non-identical pair combination $\pi^{\pm}K^0_S$ in pp collisions at $\sqrt{s} = 13$ TeV is presented for the first time to study the nature of the $K^*_0(700)$ resonance. The choice of using pp collisions for this work responds to the necessity of studying the FSI in a small system in which the strength of the FSI is expected to be more sensitive to the system size and thus to the quark nature of the resonance [7]. Due to the short-range nature of the strong interaction which might produce the resonant state, measurements in pp collisions are more suited since interparticle distances of a few fm are obtained [8]. Moreover, it has already been observed that the presence of resonances in the correlation function is enhanced for measurements in small colliding systems, since the signal-to-background for the considered state scales as $1/\text{multiplicity}$ [8].

The results presented in this Letter are obtained using data collected by the ALICE Collaboration [22,23] during the 2015–2018 pp LHC run. The Letter is organized into seven sections: Introduction, Data Analysis, Correlation Function, Fitting, Systematic uncertainties, Results and Discussion, and Summary. The Data Analysis section gives details on how the data were taken and how the $\pi^{\pm}$ and K^0_S were reconstructed and identified. The Correlation Function section describes how the $\pi^{\pm}K^0_S$ pairs were used to construct the correlation functions for this analysis. The Fitting section describes the model used to fit the correlation functions in order to extract the source parameters and FSI parameters. The Systematic uncertainties section discusses how the systematic uncertainties were calculated. The Results and Discussion section presents the results for the extracted parameters and discusses their interpretation. The Summary section summarizes the results of the present work.

2. Data analysis

The ALICE detector and its performance are described in detail in Refs. [22,24]. Collision events are selected by using the information from the V0 detectors composed of the V0C and V0A scintillator arrays [25,26], located on both sides of the interaction point, covering the pseudorapidity intervals $-3.7 < \eta < -1.6$ and $2.8 < \eta < 5.1$, respectively. In the analysis 5×10^8 minimum bias triggered pp collisions at $\sqrt{s} = 13$ TeV were used. Charged particle multiplicity classes, given in terms of multiplicity percentile intervals of the visible inelastic pp cross section, were also determined from the V0 detectors [27].

The Time Projection Chamber (TPC) [28] and the Inner Tracking System (ITS) [22] were used for charged particle tracking. These detectors cover the pseudorapidity range of $|\eta| < 0.9$ and are located within a solenoid magnet with a field strength of magnitude $B = 0.5$ T. The momentum (p) determination for charged tracks was made using only the TPC space points. The ITS provided excellent spatial resolution in determining the primary collision vertex. This vertex was used to constrain the tracks reconstructed with the TPC, requiring it to be within ± 10 of the center of the ALICE detector. The average momentum resolution typically obtained in this analysis for charged tracks was less than 10 MeV/c [24]. The selections based on the quality of track fitting [24,28,29], in addition to the standard track quality criteria [24], were used to ensure that only well-reconstructed tracks were taken into account in the analysis. The quality of the track was determined by the χ^2/N value for the Kalman fit to the particle trajectory in the TPC, where N is the number of TPC clusters attached to the track [24]. The track was rejected if the value was larger than 4.0.

Analysis specific event selection criteria were also applied. The event must have one accepted possible $\pi^{\pm}K^0_S$ pair. To reduce the effects of mini-jets which tend to produce non-flat structures in the two-particle correlation functions used in femtoscopy [30], a selection on the event transverse sphericity, calculated from the azimuthal distribution of tracks, was applied by requiring $S_T > 0.7$. S_T is a scalar quantity that takes values in the range $0 - 1$ characterizing the event shape, i.e. $S_T \sim 0$ values represent elongated events that are "jet-like" and result from a single hard-scattering of partons, whereas $S_T \sim 1$ values represent spherical "non-jet-like" events resulting from many soft parton scatterings or several hard parton scatterings. See Ref. [30] for more details. Note that the $S_T > 0.7$ selection is estimated to have $< 10\%$ effect on the multiplicity of tracks entering the femtoscopy analysis since this selection tends to remove single hard-scattering events. Pile-up events were rejected using the timing information from the V0 (for out of bunch pile-up) and multiple reconstructed vertices from tracks (or track segments in the Silicon Pixel Detector layers of the ITS) [29,30]. The possible effect due to remaining pile-up events passing the event selection criteria described above was investigated by performing the analysis using only low interaction-rate data-taking periods. No significant difference was found in the results of the analysis compared with the higher interaction-rate runs used. Both sets of runs were combined for the present analysis.

Charged particles were identified with the central barrel detectors. Particle Identification (PID) for reconstructed tracks was carried out using both the TPC and Time-Of-Flight (TOF) detectors. For the TPC, the specific ionization energy loss $\mathrm{d}E/\mathrm{d}x$ was measured, and for the TOF, the flight time of the particle in the pseudorapidity range $|\eta| < 0.9$ was measured [29,31]. For the PID signal, a value (N_σ) was assigned to each track denoting the number of standard deviations between the measured PID signal and the expected values, assuming a mass hypothesis, divided by the detector resolution for both detectors [6,24,29,31]. A parametrized Bethe-Bloch formula [24] was used for the TPC PID to calculate the expected energy loss $\langle \mathrm{d}E/\mathrm{d}x \rangle$ in the detector for a particle with a given charge, mass, and momentum. The particle mass was used to calculate the expected time-of-flight as a function of track length and momentum for the TOF PID. The detailed description of the particle identification methods is given in Ref. [32].

For Monte Carlo (MC) calculations, particles from pp collisions simulated by the general-purpose generator PYTHIA8 [33] with the Monash 2013 tune [34] were transported through a GEANT3 [35] model of the ALICE detector. The total number of simulated pp collisions used in this analysis is 5×10^8.

Table 1
$\pi^{\pm}$ and K^0_S selection criteria.

Neutral kaon selection	Value
Daughter p_T	> 0.15 GeV/c
Daughter $\|\eta\|$	< 0.8
Daughter DCA (3D) to primary vertex	> 0.4 cm
Daughter TPC PID [N_σ]	< 3
Daughter TOF PID [N_σ] (for $p > 0.8$ GeV/c)	< 3
Kalman fit χ^2/N	≤ 4
$\|\eta\|$	< 0.8
DCA (3D) between daughters	< 0.3 cm
DCA (3D) to primary vertex	< 0.3 cm
Decay length (3D, lab frame)	< 30 cm
Decay radius (2D, lab frame)	> 0.2 cm
Cosine of pointing angle	> 0.99
Invariant mass	$0.485 < m < 0.510$ GeV/c^2
Primary pion selection	**Value**
p_T	$0.15 < p_T < 1.2$ GeV/c
$\|\eta\|$	< 0.8
Transverse DCA to primary vertex	< 2.4 cm
Longitudinal DCA to primary vertex	< 3.0 cm
TOF PID [N_σ] with valid TOF signal and $p > 0.5$ GeV/c	< 2
TPC PID [N_σ] if no TOF signal for all p	< 2
Kalman fit χ^2/N	≤ 4

The methods used to select and identify individual K^0_S and $\pi^{\pm}$ particles are similar to those used for the ALICE $K^{\pm}K^0_S$ analysis in pp collisions at $\sqrt{s} = 13$ TeV [7].

K^0_S are reconstructed from their decay into $\pi^+\pi^-$, which has a branching ratio of 69% [20]. The neutral K^0_S decay vertices and parameters are reconstructed and calculated from pairs of detected $\pi^+\pi^-$ tracks, and selected based on their invariant mass and the K^0_S decay topology. The selection criteria for the K^0_S and the daughter pions are shown in Table 1.

The selection criteria are based on decay topology, i.e. distance-of-closest-approach (DCA) between charged pion daughters, DCA of daughter pion to the primary vertex, DCA of reconstructed K^0_S to the primary vertex, cosine of pointing angle, and decay length of K^0_S, and were tuned to optimize purity and statistical significance. If two reconstructed K^0_S particles share a daughter track, both are removed from the analysis. The MC samples were used to study any bias that might be induced by this procedure, which resulted in rejecting $< 1\%$ of the K^0_S candidates [6,7]. Reconstructed K^0_S candidates within invariant mass range $0.485 < m(\pi^+\pi^-) < 0.510$ GeV/c^2 are used in this analysis which gives $98 \pm 1\%$ purity of K^0_S. The purity here is defined as signal/(signal + background). The signal and background counts are calculated by fitting a fourth-order polynomial to the side-bands of the signal region to estimate the background there and subtracting this from the invariant mass histogram. A Gaussian is used to fit the signal peak in the invariant mass distribution (see Fig. 2 of Ref. [6]).

Primary charged pions are selected using the PID information from the TPC and TOF detectors. The TPC is used for PID in the full momentum range, except if a valid TOF signal is available for $p > 0.5$ GeV/c then TOF PID is used. For more details, refer to Refs. [5,6]. Table 1 summarizes the criteria used for the charged pion selection. The average charged pion purity is found using MC simulations to be $98.1 \pm 0.1\%$, in agreement with the charged pion purity reported in Ref. [6].

Two-track effects, such as the merging of two real tracks into one reconstructed track and the splitting of one real track into two reconstructed tracks, are an important challenge for femtoscopic studies. A selection on the minimum separation distance between the primary pion and a daughter pion from the decay of the K^0_S in the $\pi^{\pm}K^0_S$ pair was made from the corresponding TPC tracks using the same method as described in Ref. [7]. The distance between the two tracks was calculated in different positions along their trajectory in the TPC (at radial distances from 85 to 150 cm from the interaction point) and a minimum separation distance of 20 cm was required.

3. Measurement of correlation functions

The momentum correlations of $\pi^{\pm}K^0_S$ pairs using the two-particle correlation function are studied in this analysis. The correlation function is defined as $C(k^*) = A(k^*)/B(k^*)$, where $A(k^*)$ is the measured distribution of pairs from the same event and $B(k^*)$ is the reference distribution of pairs from mixed events. The denominator $B(k^*)$ is formed by mixing particles from one event with particles from 10 different events that satisfy the conditions that the primary vertex positions along the beam direction are within 2 cm of each other, and have similar multiplicity, i.e. events within 2% difference in multiplicity percentile are mixed. Other sizes of the mixed events buffer were also investigated with no significant effect on the results of this work. All events used are required to satisfy the $S_T > 0.7$ selection. The k^* is the magnitude of the momentum of each of the particles in the pair rest frame. In the present case of unequal mass particles in the pair, m_1 and m_2, k^* is given by

$$k^* = \sqrt{\frac{a^2 - m_1^2 m_2^2}{2a + m_1^2 + m_2^2}} \tag{1}$$

where,

$$a \equiv (q_{\text{inv}}^2 + m_1^2 + m_2^2)/2. \tag{2}$$

For convenience, the square of the invariant momentum difference $q_{\text{inv}}^2 = |\vec{p}_1 - \vec{p}_2|^2 - |E_1 - E_2|^2$ is evaluated with the momenta and energies of the two particles measured in the laboratory frame. In the case where $m_1 = m_2$, k^* can be expressed as $k^* = q_{\text{inv}}/2$. A k^* bin size of 20 MeV/c was used in the analyses presented in this Letter.

Correlation functions are analyzed for three cases: 1) $0-100\%$ multiplicity class and $k_T > 0$ GeV/c, 2) $0-100\%$ multiplicity class and $k_T < 0.5$ GeV/c, and 3) $0-5\%$ multiplicity class and $k_T < 0.5$ GeV/c, where $k_T = |\vec{p}_{T1} + \vec{p}_{T2}|/2$, and where $\vec{p}_{T1}$ and $\vec{p}_{T2}$ are the transverse momenta of the particles in the pair. The three cases correspond to the following average k_T and average charged-particle pseudorapidity density ($\langle dN/d\eta \rangle$ in the $|\eta| < 0.8$ range) values [27]: 1) $\langle k_T \rangle = 0.655$ GeV/c, $\langle dN/d\eta \rangle = 6.89$, 2) $\langle k_T \rangle = 0.323$ GeV/c, $\langle dN/d\eta \rangle = 6.89$, and 3) $\langle k_T \rangle = 0.326$ GeV/c, $\langle dN/d\eta \rangle = 21.2$. The purpose of analyzing these

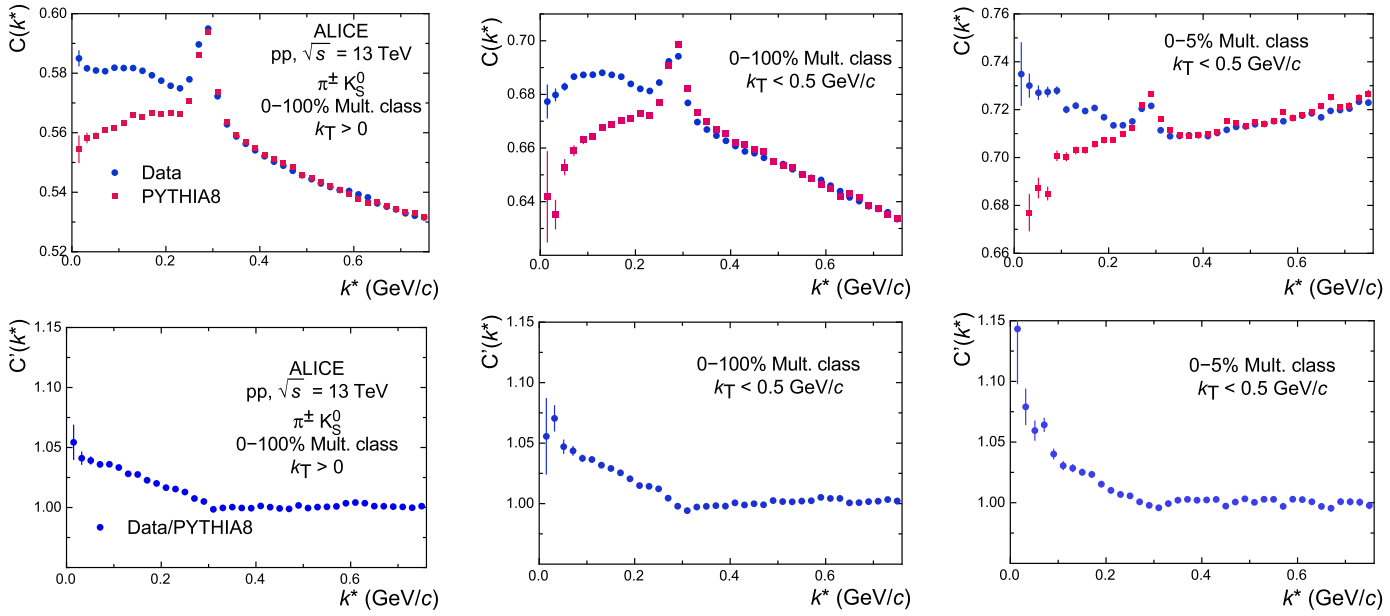

Fig. 1. Top row: $\pi^{\pm}K^0_S$ correlation functions experimentally measured (blue dots) compared with PYTHIA8+GEANT3 simulations (red squares) obtained in pp collisions at $\sqrt{s} = 13$ TeV for $0-100\%$ multiplicity class and $k_T > 0$ (left), $0-100\%$ multiplicity class and $k_T < 0.5$ GeV/c (center), and 0–5% multiplicity class and $k_T < 0.5$ GeV/c (right). The PYTHIA8+GEANT3 correlation function is normalized to the data at $k^* = 0.5$ GeV/c. Bottom row: Ratio of Data to PYTHIA8+GEANT3 simulations for the three studied cases. Statistical uncertainties are represented by bars.

cases is to obtain different femtoscopic source sizes and to study the effect of source size on the FSI. It has been found from femtoscopy measurements in pp collisions that the source size depends on both $\langle k_T \rangle$ and $\langle dN/d\eta \rangle$ [4,36]. In addition, case 1) was chosen to maximize the sample size and to provide a selection-free case to compare with the other cases having multiplicity and k_T selections.

Monte Carlo simulations were used to simulate correlation functions which were compared with experimental data. Fig. 1 shows in the top row the correlation functions experimentally measured (blue) along with the simulated ones (red). The MC correlation functions are normalized to the experimental ones at $k^* = 0.5$ GeV/c for the three cases mentioned above. The single-event and mixed-event distributions of the correlation functions are summed over $\pi^+K^0_S$ and $\pi^-K^0_S$ pairs, since it is found that there is no significant difference between the $\pi^+K^0_S$ and $\pi^-K^0_S$ corresponding correlation functions. The decay of the K*(892) meson is clearly seen at $k^* \sim 0.3$ GeV/c for all cases. For $k^* > 0.35$ GeV/c a non-flat baseline is also observed in all cases. This non-flat baseline is associated with soft parton fragmentation, or mini-jets, that are not completely suppressed by the transverse sphericity selection [36–38], as well as the presence of momentum conservation effects. Non-flat baselines in two-particle correlation functions obtained in pp collisions are often observed [9,36,37]. In particular, measured correlation functions show a decreasing dependence of the baseline with increasing k^* for low multiplicity classes, and a reversal of this dependence for higher multiplicity classes, as seen in Fig. 1. This effect in the data is seen to be present as well in the PYTHIA8 simulations. The simulations well reproduce the K*(892) peak and the background visible at larger k^*, hence in order to remove these two contributions, the measured correlation function is subsequently divided by the simulated one, defined as $C'(k^*)$, as shown in the bottom panels of Fig. 1. The statistical uncertainty from the MC correlation function is propagated with the uncertainty from the experimental one in the ratio, which becomes the final correlation function.

Finite track momentum resolution can smear the relative momentum correlation functions used in this analysis. This effect is corrected using MC simulations as done in previous works [22,23]. It is found that the effect of the momentum resolution correction is small for the very lowest k^* bin with the largest statistical error bars and negligible for the rest of the bins, resulting in a $< 3\%$ effect on the extracted fit parameters.

4. Fitting

The momentum resolution corrected ratio of the experimental $\pi^{\pm}K^0_S$ correlation function to the MC correlation function was fitted by a model in order to extract information on the size of the source, as well as the strength and nature of the FSI between the particles in the pair. The fit function is given by,

$$C'(k^*) = \kappa \left[C_{\text{Lednicky}}(k^*) + \varepsilon \frac{dN_{BW}}{dm} \frac{dm}{dk^*} \right] \tag{3}$$

where,

$$\frac{dN_{BW}}{dm} \propto \frac{\Gamma_{892}}{(m - m_{892})^2 + \Gamma^2_{892}/4} \tag{4}$$

is the Breit–Wigner resonance distribution. This last term fits out any residual presence of the K*(892) peak (see below).

The quantities ε and κ, where ε is the magnitude of a correction term on the MC modeling of the K*(892) (see below) and κ is an overall normalization factor, are fit parameters, and Γ_{892} and m_{892} are the full-width at half maximum (FWHM) and mass of the K*(892), respectively, taken from the Review of Particle Physics [20]. The first term in Eq. (3) is a modified version of the Lednicky parametrization [2,39,40] which assumes that the pair interaction is due to strong final-state interaction of a near-threshold resonance. The second term in Eq. (3) is used to fit out the small residual bump in the ratio that results from a slight overcompensation of the MC in modeling the K*(892) peak in the data that can be seen in Fig. 1, located at $k^* \sim 0.3$ GeV/c. Fitting out this residual bump results in an improved χ^2/ndf for all of the fits.

A Gaussian distribution of the source size in the pair reference frame is assumed in the FSI parameterization. More general forms for this distribution could be used, but using the Gaussian results in the analytic form of the Lednicky equation. Another motivation for staying with the Gaussian is to facilitate comparisons with previous published results that also used the Gaussian distribution.

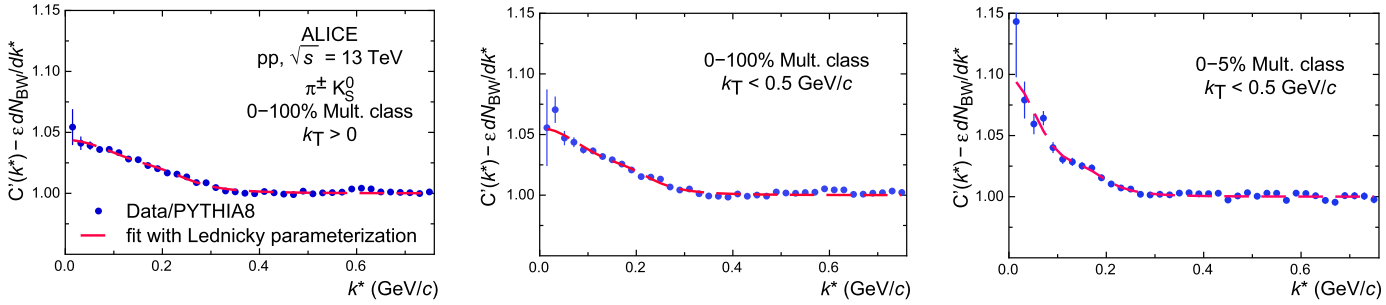

Fig. 2. Example fit of Eq. (5) to the corrected correlation functions after Eq. (3) has been used to remove the PYTHIA8+GEANT3 overcompensation of the K*(892), for $\pi^{\pm}\mathrm{K}^0_\mathrm{S}$ from $\sqrt{s} = 13$ TeV pp collisions for 0 – 100% multiplicity class and $k_T > 0$ (left), 0 – 100% multiplicity class and $k_\mathrm{T} < 0.5$ GeV/c (center), and 0–5% multiplicity class and $k_\mathrm{T} < 0.5$ GeV/c (right). Statistical uncertainties are represented as bars.

The quantity $C_{\mathrm{Lednicky}}(k^*)$ has the form

$$C_{\mathrm{Lednicky}}(k^*) = 1 + \left(\frac{\lambda\alpha}{2}\right)\left[\left|\frac{f(k^*)}{R}\right|^2 + \frac{4\mathcal{R}f(k^*)}{\sqrt{\pi}R}F_1(2k^*R) - \frac{2\mathcal{I}f(k^*)}{R}F_2(2k^*R) + \Delta C\right] \quad (5)$$

and

$$F_1(z) = \int_0^z dx\,\frac{e^{x^2-z^2}}{z}; \quad F_2(z) = \frac{1-e^{-z^2}}{z}. \quad (6)$$

α is the symmetry parameter and is set to 0.5 assuming symmetry in K^0 and $\overline{\mathrm{K}^0}$ production since the K^0_S is a linear combination of these; R is the radius parameter of the source; and λ is the correlation strength. The term $f(k^*)$ is the s-wave $\pi^{\pm}\mathrm{K}^0_\mathrm{S}$ scattering amplitude whose FSI contribution is the near-threshold resonance. A relativistic Breit–Wigner amplitude is assumed,

$$f(k^*) = \frac{\gamma}{M_R^2 - s - i\gamma k^*}. \quad (7)$$

In Eq. (7), M_R is the mass of the resonance, and γ is the coupling of the resonance to its decay channel, i.e. $\pi^{\pm}\mathrm{K}^0_\mathrm{S}$. Also, $s = (\sqrt{m_\mathrm{K}^2 + k^{*2}} + \sqrt{m_\pi^2 + k^{*2}})^2$ is the square of the energy of the pair in its rest frame. A Breit–Wigner form was chosen for $f(k^*)$ since the fitted M_R and γ to the FSI resonance from the present work will be compared with other measurements that used the Breit–Wigner form in order to identify the resonance [41,42].

The quantity ΔC is a correction to the derivation of Eq. (5), that assumes spherical outgoing waves, to account for the true scattered waves in the inner region of the short-range potential [2,7], and is given by,

$$\Delta C = \frac{(2 + m_\pi/m_\mathrm{K} + m_\mathrm{K}/m_\pi)}{2\sqrt{\pi}R^3\gamma}|f(k^*)|^2. \quad (8)$$

As a test, a p-wave term was added to the s-wave term in the scattering amplitude in deriving the Lednicky equation to study whether there was interference of the K*(892) with the s-wave FSI. It was found that the p-wave term had a negligible effect on the fits, and was thus ignored.

The fitting strategy was to make a six-parameter fit of Eq. (3) to the corrected ratio of the experimental $\pi^{\pm}\mathrm{K}^0_\mathrm{S}$ correlation function to the corresponding MC correlation function to extract R, λ, M_R, γ, ε, and κ. The nominal fit range is $0 < k^* < 0.76$ GeV/c in all cases. The nominal maximum of 0.76 GeV/c of the fit range was set to give the optimal overlap between the experimental and MC correlation functions in the baseline region.

Fig. 2 shows the correlation functions and fits. The MC overcompensation of the K*(892) has been removed from the "Data/MC" points by subtracting out the second term in Eq. (3) in order to show how well $C_{\mathrm{Lednicky}}(k^*)$ fits the ratio, and the ratio has been divided by κ. The χ^2/ndf for the fits shown in Fig. 2 are 1.6, 1.8, and 0.92, with p-values of 1.7% and 0.36% and 60%, respectively.

5. Systematic uncertainties

Table 2 shows the total systematic uncertainties on the R, λ M_R, and γ parameters extracted from the $\pi^{\pm}\mathrm{K}^0_\mathrm{S}$ correlation function in pp collisions at $\sqrt{s} = 13$ TeV.

The "fit systematic uncertainty" column reports the systematic uncertainty due to varying the k^* fit range. Varying the fit range by 20% resulted in < 3% effect on the fit parameters. Fitting uncertainties were calculated including correlations among the fit parameters as done using a MINOS algorithm in order to obtain conservative estimates of the uncertainties [43].

The "selection systematic uncertainty" column reports the systematic uncertainty related to the variation of track and PID selection criteria used in the data analysis. To determine this, the single particle selection criteria shown in Table 1 were varied by ±10%, and the value chosen for the minimum separation distance of same-sign tracks was varied by ±20% [7]. The systematic uncertainty related to the sphericity selection of $S_\mathrm{T} > 0.7$ is also included in this source of systematic uncertainty, where S_T was varied by ±10% from its nominal selection value. The uncertainty was estimated from the variation of the results with respect to those obtained with the nominal selections. The resulting relative systematic uncertainties are of about 10% for λ, about 5% for R, and about 2% for the other parameters.

The "total systematic uncertainty" column is obtained as the sum in quadrature of the contribution of the two sources described above. The "total uncertainty" column is the sum in quadrature of the statistical uncertainty and the total systematic uncertainty. As seen, the total systematic uncertainties tend to be greater than or comparable to the statistical uncertainties. Table 3 shows an approximate breakdown of the relative systematic uncertainties (in percentage) from the different variations considered. See Table 1 in Section 2 for the nominal values of the selection criteria. Note that "min. sep. var." refers to the variation of the selection for minimum separation between K^0_S daughter and primary pions in the TPC, mentioned earlier, and "$m(\pi^+\pi^-)$ and primary vertex variations" refer to the combined effect of varying the invariant mass selection for K^0_S and varying the selection for the primary vertex of the event. As seen, in general the variations have the largest effect on λ and the smallest effect on M_R and γ, with the S_T variation having the largest single-variation effect on all of the parameters.

6. Results and discussion

The R, λ, M_R, and γ parameters extracted from the present analysis of $\pi^{\pm}\mathrm{K}^0_\mathrm{S}$ correlation functions in pp collisions at $\sqrt{s} = 13$ TeV are reported in Table 2 for the three cases mentioned above. The λ parame-

Table 2
Fit results for R, λ, M_R, and γ showing statistical and systematic uncertainties from the present analysis. Uncertainties are symmetric unless specified otherwise. See the text for the description of the various sources of uncertainties.

R, λ, M_R, or γ	fit value	statistical uncertainty	fit systematic uncertainty	selection systematic uncertainty	total systematic uncertainty	total uncertainty
0 – 100% multiplicity class $k_T > 0$						
R (fm)	0.912	0.037	0.011	0.053	0.054	0.065
λ	0.0783	+0.0096 -0.0086	0.0032	0.0078	0.0084	+0.0127 -0.0121
M_R (GeV/c^2)	0.833	0.002	0.006	0.013	0.015	0.015
γ (GeV)	0.890	0.015	0.012	0.016	0.020	0.025
0 – 100% multiplicity class $k_T < 0.5$ GeV/c						
R (fm)	1.063	0.058	0.015	0.064	0.066	0.088
λ	0.111	0.017	0.004	0.013	0.014	0.022
M_R (GeV/c^2)	0.804	0.003	0.005	0.013	0.014	0.014
γ (GeV)	0.801	0.023	0.020	0.014	0.024	0.033
0 – 5% multiplicity class $k_T < 0.5$ GeV/c						
R (fm)	1.618	+0.136 -0.109	0.015	0.089	0.090	+0.163 -0.142
λ	0.274	+0.077 -0.053	0.001	0.026	0.026	+0.081 -0.059
M_R (GeV/c^2)	0.765	0.004	0.002	0.012	0.013	0.013
γ (GeV)	0.714	+0.042 -0.037	0.005	0.013	0.014	+0.044 -0.039

Table 3
Breakdown of the relative systematic uncertainties for R, λ, M_R, and γ from the variation of track, PID and mixed-event selection criteria. The %Δ row is the percentage that the quantity was changed. See the text for the description of the various uncertainties.

Quantity changed	Fit range	Min. sep. var.	TOF, TPC N_σ	DCA var.	$m(\pi^+\pi^-)$ and primary vertex var.	Multiplicity difference for event mixing	Decay length	S_T var.
%Δ	20	20	10	10	10	10	10	10
%R	1	1	2	2	1	1	1	3
%λ	3	5	3	3	3	2	2	5
%M_R	1	< 1	< 1	< 1	< 1	< 1	< 1	2
%γ	2	1	< 1	< 1	< 1	< 1	< 1	2

ters are corrected for purity by dividing the extracted λ values with the product of the $\pi^\pm$ and K^0_S purities (see Section 2).

Since the main goal of this measurement is to study the $K^*_0(700)$ resonance, one must first establish that the FSI of the $\pi^\pm K^0_S$ pair occurs indeed through this resonance. This can be done by comparing the measured M_R and γ parameters extracted from this analysis with previously measured values of M_R and Γ_R for the $K^*_0(700)$ [41,42], where Γ_R is the FWHM of the relativistic Breit–Wigner resonance distribution, whose amplitude is expressed as [44],

$$f(s) \sim \frac{1}{M_R^2 - s - iM_R\Gamma_R}. \tag{9}$$

Comparing this denominator with the denominator of Eq. (7), one can obtain an estimate for Γ_R from the present results,

$$\Gamma_R = \frac{\langle k^* \rangle \gamma}{M_R}, \tag{10}$$

where $\langle k^* \rangle$ is the average of k^* determined by weighting k^* by the experimental dN/dk^* distribution over the fit range used in fitting Eq. (3) to the correlation function. Table 4 lists the values of Γ_R extracted from the present work using Eq. (10) for the three cases studied. The uncertainties shown for $\langle k^* \rangle$ are estimated by considering different k^* ranges for calculating the average, namely $0 < k^* < 0.6$ GeV/c and $0 < k^* < 2$ GeV/c, and taking the differences from the nominal $\langle k^* \rangle$ to obtain conservative estimates of the uncertainties.

Table 4
The $\langle k^* \rangle$ and corresponding Γ_R extracted from the three cases measured in the present work using Eq. (10).

Case	$\langle k^* \rangle$ (GeV/c)	Γ_R (GeV/c^2)
0 – 100% multiplicity class, $k_T > 0$	$0.403^{+0.093}_{-0.056}$	$0.430^{+0.088}_{-0.053}$
0 – 100% multiplicity class, $k_T < 0.5$ GeV/c	$0.408^{+0.060}_{-0.050}$	$0.406^{+0.050}_{-0.042}$
0 – 5% multiplicity class, $k_T < 0.5$ GeV/c	$0.418^{+0.072}_{-0.053}$	$0.390^{+0.068}_{-0.051}$

Fig. 3 compares the values of M_R and Γ_R extracted in the present work with measurements of these quantities for the $K^*_0(700)$ from the BES [41] and E791 Collaborations [42]. The BES Collaboration measured the relativistic Breit–Wigner parameters of the $K^*_0(700)$ through the decay of the J/ψ meson, whereas the E791 Collaboration measured them through the decay of the D^+ meson. The total uncertainties defined as the quadratic sum of the statistical and systematic uncertainties are shown on the points for all cases. As seen, the values reported in this work agree within uncertainties with the $K^*_0(700)$ Breit–Wigner param-

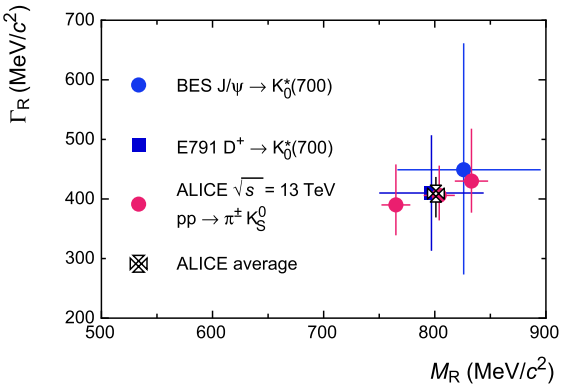

Fig. 3. The extracted Breit–Wigner parameters from the $\pi^{\pm}K^0_S$ femtoscopic correlation in pp collisions at $\sqrt{s} = 13$ TeV compared with those for $K^*_0(700)$ from the BES [41] and the E791 [42] experiments. The horizontal and vertical bars represent the total uncertainties. The "ALICE average" value is the weighted average of the three ALICE points.

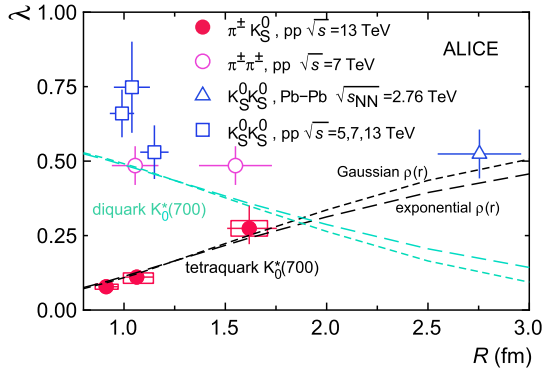

Fig. 4. The λ parameter as a function of source size R extracted from the $\pi^{\pm}K^0_S$ femtoscopy measurement in pp collisions at $\sqrt{s} = 13$ TeV. Results are compared with the previous ALICE measurements, obtained from $K^0_S K^0_S$ [6,7] and $\pi\pi$ [36] femtoscopy studies in pp and Pb–Pb collisions and the calculations from a toy geometric model (see text). The model calculations for the tetraquark and diquark hypotheses for the $K^*_0(700)$ are shown as black and light green dashed lines, respectively, the short dashed lines representing the Gaussian $\rho(r)$ and the long dashed lines representing the exponential $\rho(r)$.

eters measured in the other two experiments. It is seen that the present results have smaller uncertainties than the previous measurements. It is also seen that although the three Γ_R values from the present work agree within uncertainties, the differences among the three M_R values are outside of their uncertainties. This could be a consequence of using the Breit–Wigner function to fit a resonance where the condition $\Gamma_R \ll M_R$ is not fulfilled, which can lead to kinematic dependences on the extracted M_R and Γ_R [20,44]. However, these differences in M_R are small compared with the extracted M_R values, and thus it is judged that these results strongly support the assumption that the resonance responsible for the FSI of the $\pi^{\pm}K^0_S$ pairs studied in the present work is the $K^*_0(700)$ resonance.

The extracted R and λ parameters shown in Table 2 can be used to obtain information about the quark configuration of the $K^*_0(700)$. Fig. 4 compares the values of R and λ extracted in the present work with published results for these parameters from ALICE measurements in pp and Pb–Pb collisions in which $\pi\pi$ and $K^0_S K^0_S$ pairs were analyzed [4,6,7,36]. The $\pi^{\pm}K^0_S$ results are shown with separate statistical (error bars) and systematic (boxes) uncertainties, whereas for the previous results, the error bars represent the combination of the statistical and systematic uncertainties. For the $\pi\pi$ femtoscopic measurements in pp collisions at $\sqrt{s} = 7$ TeV reported in [36] with average k_T values of ~ 0.15 and ~ 0.35 GeV/c, the λ values are given as varying in the range $0.42 - 0.55$, so λ is plotted as the center of this range with uncertainties extending to the upper and lower limits of the range.

For the R parameter, the values from the present $\pi^{\pm}K^0_S$ analysis are comparable with the published $\pi\pi$ and $K^0_S K^0_S$ measurements in pp collisions, i.e. in the range 1–2 fm, as would be expected from pp collisions where the source size is ~ 1 fm. For the λ parameter, whereas the results from $\pi\pi$ and $K^0_S K^0_S$ are compatible with values of about 0.5 or greater, for the present $\pi^{\pm}K^0_S$ analysis significantly lower values are obtained, ranging from about 0.05 to about 0.25 depending on R. The expectation is that λ would be the same for $\pi^{\pm}K^0_S$ as for the identical-meson measurements. The λ value of ~ 0.5 has been shown to be due to the presence of long-lived resonances whose decay into the detected mesons impacts the measurement of the "direct" mesons coming from the source of interest [7,45]. Another significant difference between the present $\pi^{\pm}K^0_S$ results and the $\pi\pi$ and $K^0_S K^0_S$ results is that λ has a strong R dependence for the former, whereas there is no significant dependence of λ on R for the latter, i.e. even extending R to the value from Pb–Pb collisions shows no significant effect on λ.

As discussed in Refs. [7] and [9], a physics effect that could cause this difference in λ values for $\pi^{\pm}K^0_S$ pairs is related to the possibility that the $K^*_0(700)$ resonance, that is assumed to be solely responsible for the FSI in the $\pi^{\pm}K^0_S$ pair, is actually a tetraquark state of the form $(q_1, \bar{q_2}, q_3, \bar{q_3})$, in which q_1, q_2 and q_3 indicate the flavor of the valence quarks of the π and K^0_S. In particular, q_1 and q_2 can be a u or s quark, while q_3 is a d quark. For example, the quark content of a tetraquark $K^*_0(700)^+$ would be $u\bar{s}d\bar{d}$, whereas the diquark version would be $u\bar{s}$. The strength of the FSI through a tetraquark $K^*_0(700)^+$ could be decreased by the small source size of the $\pi^{\pm}K^0_S$ source, i.e. at $R \sim 1$ fm as is measured in these collisions. This could occur since $d-\bar{d}$ annihilation would be enhanced due to the proximity of the $\pi^{\pm}$ and K^0_S at their creation, which would open up a non-resonant channel in the scattering process that would be reflected by reducing λ. For a FSI through a diquark $K^*_0(700)^+$, with the form $u\bar{s}$, the small source geometry should not reduce its strength. For the $K^0_S K^0_S$ and $\pi\pi$ cases, λ should not be affected by the source size since the pair correlation is dominated by the effect of quantum statistics, for which in the ideal case λ does not depend on R, and which is found to be much stronger than the strong FSI present for these identical particle pairs [2].

In order to demonstrate the R dependence of λ for a tetraquark or a diquark $K^*_0(700)$ based on the geometric considerations discussed above, a simple toy model is constructed, taking the form of the λ factor for a tetraquark state,

$$\lambda = \lambda_0(1 - aP) \tag{11}$$

and for a diquark,

$$\lambda = \lambda_0 aP \tag{12}$$

where,

$$P \equiv \frac{\int \rho(r)\rho(|\vec{r} - \vec{R}|)dV}{\int |\rho(r)|^2 dV} \tag{13}$$

can be considered the "overlap probability" between the π and K^0_S in the pair as they are emitted from the pp collision. The quantity $\rho(r)$ is the meson volume distribution, assumed to be the same for the π and K^0_S, λ_0 is the maximum value for λ, and a is essentially the "$d-\bar{d}$ annihilation efficiency" that in principle could take any value in the range $0 - 1$. Assuming $\rho(r) \sim e^{-r^2/(2\sigma^2)}$ or $\sim e^{-r/r_0}$, $\lambda_0 = 0.6$, the average value for $\pi\pi$ and $K^0_S K^0_S$ measurements from Refs. [36] and [6,7], and assuming 100% $d-\bar{d}$ annihilation efficiency for any non-zero overlap, $a = 1$, the free parameters of the model, i.e. σ and r_0, are adjusted to give a good fit to the $\pi^{\pm}K^0_S$ measurements. The results from Eqs. (11) and (12) are shown in Fig. 4, along with the results from $\pi^{\pm}K^0_S$ measurements of this work and

published ALICE measurements for $K^0_S K^0_S$ [6,7] and $\pi\pi$ pairs [36] from pp and Pb–Pb collisions. The free model parameters are set to $\sigma = 1.1$ fm and $r_0 = 0.85$ fm for the Gaussian (short dashed lines) and exponential (long dashed lines) distributions, respectively, which are considered reasonable values since hadronic sizes are expected to be ~ 1 fm. As seen, using reasonable model parameter values, the tetraquark case, Eq. (11), describes the R dependence of λ from the present measurements well for both the Gaussian and exponential meson shapes as being a geometric effect. The diquark case is seen to predict an R dependence that is incompatible with the measured one.

Therefore, the present results of $\pi^{\pm}K^0_S$ femtoscopy in pp collisions at $\sqrt{s} = 13$ TeV suggest that the $K^*_0(700)$ is a tetraquark state.

7. Summary

Femtoscopic correlations with the particle pair combination $\pi^{\pm}K^0_S$ are studied in pp collisions at $\sqrt{s} = 13$ TeV for the first time by the ALICE experiment at the LHC. Source parameters and final-state interaction parameters are extracted by fitting a model based on a Gaussian distribution of the source to the experimental two-particle correlation functions. The model used assumes that solely the final-state interaction through a resonance determines the correlations, and is defined in terms of a mass and the coupling parameter to the decay into a $\pi^{\pm}K^0_S$ pair. The extracted mass and width parameters of the FSI are consistent with previous measurements of the $K^*_0(700)$ resonance, and the smaller value and increasing behavior of the λ parameter with R compared with identical boson measurements give support that the $K^*_0(700)$ is a four-quark state, i.e. a tetraquark state [19]. A simple geometric model that assumes a tetraquark FSI describes well the R dependence of λ extracted from the measured correlation functions.

Declaration of competing interest

The authors declare that they have no known competing financial interests or personal relationships that could have appeared to influence the work reported in this paper.

Data availability

This manuscript has associated data in a HEPData repository at: https://www.hepdata.net/record/ins2739149.

Acknowledgements

The ALICE Collaboration would like to thank all its engineers and technicians for their invaluable contributions to the construction of the experiment and the CERN accelerator teams for the outstanding performance of the LHC complex. The ALICE Collaboration gratefully acknowledges the resources and support provided by all Grid centres and the Worldwide LHC Computing Grid (WLCG) collaboration. The ALICE Collaboration acknowledges the following funding agencies for their support in building and running the ALICE detector: A. I. Alikhanyan National Science Laboratory (Yerevan Physics Institute) Foundation (ANSL), State Committee of Science and World Federation of Scientists (WFS), Armenia; Austrian Academy of Sciences, Austrian Science Fund (FWF): [M 2467-N36] and Nationalstiftung für Forschung, Technologie und Entwicklung, Austria; Ministry of Communications and High Technologies, National Nuclear Research Center, Azerbaijan; Conselho Nacional de Desenvolvimento Científico e Tecnológico (CNPq), Financiadora de Estudos e Projetos (Finep), Fundação de Amparo à Pesquisa do Estado de São Paulo (FAPESP) and Universidade Federal do Rio Grande do Sul (UFRGS), Brazil; Bulgarian Ministry of Education and Science, within the National Roadmap for Research Infrastructures 2020-2027 (object CERN), Bulgaria; Ministry of Education of China (MOEC), Ministry of Science & Technology of China (MSTC) and National Natural Science Foundation of China (NSFC), China; Ministry of Science and Education and Croatian Science Foundation, Croatia; Centro de Aplicaciones Tecnológicas y Desarrollo Nuclear (CEADEN), Cubaenergía, Cuba; The Ministry of Education, Youth and Sports of the Czech Republic, Czech Republic; The Danish Council for Independent Research | Natural Sciences, the Villum Fonden and Danish National Research Foundation (DNRF), Denmark; Helsinki Institute of Physics (HIP), Finland; Commissariat à l'Énergie Atomique (CEA) and Institut National de Physique Nucléaire et de Physique des Particules (IN2P3) and Centre National de la Recherche Scientifique (CNRS), France; Bundesministerium für Bildung und Forschung (BMBF) and GSI Helmholtzzentrum für Schwerionenforschung GmbH, Germany; General Secretariat for Research and Technology, Ministry of Education, Research and Religions, Greece; National Research, Development and Innovation Office, Hungary; Department of Atomic Energy, Government of India (DAE), Department of Science and Technology, Government of India (DST), University Grants Commission, Government of India (UGC) and Council of Scientific and Industrial Research (CSIR), India; National Research and Innovation Agency - BRIN, Indonesia; Istituto Nazionale di Fisica Nucleare (INFN), Italy; Japanese Ministry of Education, Culture, Sports, Science and Technology (MEXT) and Japan Society for the Promotion of Science (JSPS) KAKENHI, Japan; Consejo Nacional de Ciencia (CONACYT) y Tecnología, through Fondo de Cooperación Internacional en Ciencia y Tecnología (FONCICYT) and Dirección General de Asuntos del Personal Académico (DGAPA), Mexico; Nederlandse Organisatie voor Wetenschappelijk Onderzoek (NWO), Netherlands; The Research Council of Norway, Norway; Commission on Science and Technology for Sustainable Development in the South (COMSATS), Pakistan; Pontificia Universidad Católica del Perú, Peru; Ministry of Education and Science, National Science Centre and WUT ID-UB, Poland; Korea Institute of Science and Technology Information and National Research Foundation of Korea (NRF), Republic of Korea; Ministry of Education and Scientific Research, Institute of Atomic Physics, Ministry of Research and Innovation and Institute of Atomic Physics and Universitatea Nationala de Stiinta si Tehnologie Politehnica Bucuresti, Romania; Ministry of Education, Science, Research and Sport of the Slovak Republic, Slovakia; National Research Foundation of South Africa, South Africa; Swedish Research Council (VR) and Knut and Alice Wallenberg Foundation (KAW), Sweden; European Organization for Nuclear Research, Switzerland; Suranaree University of Technology (SUT), National Science and Technology Development Agency (NSTDA) and National Science, Research and Innovation Fund (NSRF via PMU-B B05F650021), Thailand; Turkish Energy, Nuclear and Mineral Research Agency (TENMAK), Turkey; National Academy of Sciences of Ukraine, Ukraine; Science and Technology Facilities Council (STFC), United Kingdom; National Science Foundation of the United States of America (NSF) and United States Department of Energy, Office of Nuclear Physics (DOE NP), United States of America. In addition, individual groups or members have received support from: Czech Science Foundation (grant no. 23-07499S), Czech Republic; European Research Council, Strong 2020 - Horizon 2020 (grant nos. 950692, 824093), European Union; ICSC - Centro Nazionale di Ricerca in High Performance Computing, Big Data and Quantum Computing, European Union - NextGenerationEU; Academy of Finland (Center of Excellence in Quark Matter) (grant nos. 346327, 346328), Finland.

References

[1] M.A. Lisa, S. Pratt, R. Soltz, U. Wiedemann, Femtoscopy in relativistic heavy ion collisions, Annu. Rev. Nucl. Part. Sci. 55 (2005) 357–402, arXiv:nucl-ex/0505014 [nucl-ex].

[2] STAR Collaboration, B.I. Abelev, et al., Neutral kaon interferometry in Au+Au collisions at $\sqrt{s_{NN}} = 200$ GeV, Phys. Rev. C 74 (2006) 054902, arXiv:nucl-ex/0608012 [nucl-ex].

[3] PHENIX Collaboration, A. Adare, et al., Systematic study of charged-pion and kaon femtoscopy in Au + Au collisions at $\sqrt{s_{NN}} = 200$ GeV, Phys. Rev. C 92 (2015) 034914, arXiv:1504.05168 [nucl-ex].

[4] ALICE Collaboration, B. Abelev, et al., $K^0_s - K^0_s$ correlations in pp collisions at $\sqrt{s} = 7$ TeV from the LHC ALICE experiment, Phys. Lett. B 717 (2012) 151–161, arXiv:1206.2056 [hep-ex].

[5] ALICE Collaboration, B. Abelev, et al., Charged kaon femtoscopic correlations in pp collisions at $\sqrt{s} = 7$ TeV, Phys. Rev. D 87 (2013) 052016, arXiv:1212.5958 [hep-ex].

[6] ALICE Collaboration, J. Adam, et al., One-dimensional pion, kaon, and proton femtoscopy in Pb–Pb collisions at $\sqrt{s_{\rm NN}} = 2.76$ TeV, Phys. Rev. C 92 (2015) 054908, arXiv:1506.07884 [nucl-ex].

[7] ALICE Collaboration, S. Acharya, et al., $\rm K^0_s K^0_s$ and $\rm K^0_s K^\pm$ femtoscopy in pp collisions at $\sqrt{s} = 5.02$ and 13 TeV, Phys. Lett. B 833 (2022) 137335, arXiv:2111.06611 [nucl-ex].

[8] L. Fabbietti, V. Mantovani Sarti, O. Vazquez Doce, Study of the strong interaction among hadrons with correlations at the LHC, Annu. Rev. Nucl. Part. Sci. 71 (2021) 377–402, arXiv:2012.09806 [nucl-ex].

[9] ALICE Collaboration, S. Acharya, et al., Measuring $\rm K^0_S K^\pm$ interactions using pp collisions at $\sqrt{s} = 7$ TeV, Phys. Lett. B 790 (2019) 22–34, arXiv:1809.07899 [nucl-ex].

[10] ALICE Collaboration, S. Acharya, et al., Measuring $\rm K^0_S K^\pm$ interactions using Pb–Pb collisions at $\sqrt{s_{\rm NN}} = 2.76$ TeV, Phys. Lett. B 774 (2017) 64–77, arXiv:1705.04929 [nucl-ex].

[11] E. Santopinto, G. Galata, Spectroscopy of tetraquark states, Phys. Rev. C 75 (2007) 045206, arXiv:hep-ph/0605333 [hep-ph].

[12] R.L. Jaffe, Multi-quark hadrons. 1. The phenomenology of $\rm qq\overline{qq}$ mesons, Phys. Rev. D 15 (1977) 267.

[13] M.G. Alford, R.L. Jaffe, Insight into the scalar mesons from a lattice calculation, Nucl. Phys. B 578 (2000) 367–382, arXiv:hep-lat/0001023 [hep-lat].

[14] S. Narison, Light scalar mesons in QCD, Nucl. Phys. B, Proc. Suppl. 186 (2009) 306–311, arXiv:0811.0563 [hep-ph].

[15] N. Achasov, A. Kiselev, Light scalar mesons and two-kaon correlation functions, Phys. Rev. D 97 (2018) 036015, arXiv:1711.08777 [hep-ph].

[16] K. Azizi, B. Barsbay, H. Sundu, Light scalar $K_0^*(700)$ meson in vacuum and a hot medium, Phys. Rev. D 100 (2019) 094041, arXiv:1909.00716 [hep-ph].

[17] Hadron Spectrum Collaboration, J.J. Dudek, R.G. Edwards, D.J. Wilson, An a_0 resonance in strongly coupled $\pi\eta$, $K\overline{K}$ scattering from lattice QCD, Phys. Rev. D 93 (2016) 094506, arXiv:1602.05122 [hep-ph].

[18] R.A. Briceno, J.J. Dudek, R.G. Edwards, D.J. Wilson, Isoscalar $\pi\pi$ scattering and the σ meson resonance from QCD, Phys. Rev. Lett. 118 (2017) 022002, arXiv:1607.05900 [hep-ph].

[19] F.-K. Guo, L. Liu, U.-G. Meissner, P. Wang, Tetraquarks, hadronic molecules, meson-meson scattering and disconnected contributions in lattice QCD, Phys. Rev. D 88 (2013) 074506, arXiv:1308.2545 [hep-lat].

[20] Particle Data Group Collaboration, R.L. Workman, et al., Review of particle physics, PTEP 2022 (2022), 083C01.

[21] T.J. Humanic, Feasibility of studying the $\rm K_0^*(700)$ resonance using $\rm \pi^\pm K^0_S$ femtoscopy, J. Phys. G 46 (2019) 055001, arXiv:1810.10959 [hep-ph].

[22] ALICE Collaboration, K. Aamodt, et al., The ALICE experiment at the CERN LHC, J. Instrum. 3 (2008) S08002.

[23] ALICE Collaboration, The ALICE experiment – a journey through QCD, arXiv e-prints, arXiv:2211.04384 [nucl-ex], Nov. 2022.

[24] ALICE Collaboration, B. Alessandro, et al., ALICE: physics performance report, volume II, J. Phys. G 32 (2006) 1295–2040.

[25] ALICE Collaboration, B. Abelev, et al., Centrality dependence of π, K, p production in Pb–Pb collisions at $\sqrt{s_{\rm NN}} = 2.76$ TeV, Phys. Rev. C 88 (2013) 044910, arXiv:1303.0737 [hep-ex].

[26] ALICE Collaboration, B. Abelev, et al., Centrality determination of Pb–Pb collisions at $\sqrt{s_{\rm NN}} = 2.76$ TeV with ALICE, Phys. Rev. C 88 (2013) 044909, arXiv:1301.4361 [nucl-ex].

[27] ALICE Collaboration, S. Acharya, et al., Pseudorapidity distributions of charged particles as a function of mid- and forward rapidity multiplicities in pp collisions at $\sqrt{s} = 5.02$, 7 and 13 TeV, Eur. Phys. J. C 81 (2021) 630, arXiv:2009.09434 [nucl-ex].

[28] J. Alme, et al., The ALICE TPC, a large 3-dimensional tracking device with fast readout for ultra-high multiplicity events, Nucl. Instrum. Methods A 622 (2010) 316–367, arXiv:1001.1950 [physics.ins-det].

[29] ALICE Collaboration, B.B. Abelev, et al., Performance of the ALICE experiment at the CERN LHC, Int. J. Mod. Phys. A 29 (2014) 1430044, arXiv:1402.4476 [nucl-ex].

[30] ALICE Collaboration, S. Acharya, et al., Event-shape and multiplicity dependence of freeze-out radii in pp collisions at $\sqrt{s} = 7$ TeV, J. High Energy Phys. 09 (2019) 108, arXiv:1901.05518 [nucl-ex].

[31] A. Akindinov, et al., Performance of the ALICE time-of-flight detector at the LHC, Eur. Phys. J. Plus 128 (2013) 44.

[32] ALICE Collaboration, K. Aamodt, π^0 and η reconstruction from photon conversions in ALICE for first pp collisions at the LHC, J. Phys. Conf. Ser. 270 (2011) 012035.

[33] T. Sjostrand, S. Mrenna, P. Skands, PYTHIA 6.4 physics and manual, J. High Energy Phys. 05 (2006) 026, arXiv:hep-ph/0603175.

[34] P. Skands, S. Carrazza, J. Rojo, Tuning PYTHIA 8.1: the Monash 2013 tune, Eur. Phys. J. C 74 (2014) 3024, arXiv:1404.5630 [hep-ph].

[35] R. Brun, F. Bruyant, F. Carminati, S. Giani, M. Maire, A. McPherson, G. Patrick, L. Urban, GEANT detector description and simulation tool, CERN-W5013 1 (1994) 1.

[36] ALICE Collaboration, K. Aamodt, et al., Femtoscopy of pp collisions at $\sqrt{s} = 0.9$ and 7 TeV at the LHC with two-pion Bose-Einstein correlations, Phys. Rev. D 84 (2011) 112004, arXiv:1101.3665 [hep-ex].

[37] ALICE Collaboration, S. Acharya, et al., Scattering studies with low-energy kaon-proton femtoscopy in proton-proton collisions at the LHC, Phys. Rev. Lett. 124 (2020) 092301, arXiv:1905.13470 [nucl-ex].

[38] ALICE Collaboration, S. Acharya, et al., Experimental evidence for an attractive p-ϕ interaction, Phys. Rev. Lett. 127 (2021) 172301, arXiv:2105.05578 [nucl-ex].

[39] R. Lednicky, V. Lyuboshits, Final state interaction effect on pairing correlations between particles with small relative momenta, Sov. J. Nucl. Phys. 35 (1982) 770.

[40] R. Lednicky, Correlation femtoscopy, Nucl. Phys. A 774 (2006) 189–198, arXiv:nucl-th/0510020 [nucl-th].

[41] BES Collaboration, M. Ablikim, et al., Observation of charged κ in $J/\psi \to K^*(892)^\pm K_s \pi^\pm$, $K^*(892)^\pm \to K_s \pi^\pm$ at BESII, Phys. Lett. B 698 (2011) 183–190, arXiv:1008.4489 [hep-ex].

[42] E791 Collaboration, E.M. Aitala, et al., Dalitz plot analysis of the decay $D^+ \to K^-\pi^+\pi^+$ and the study of the $K\pi$ scalar amplitudes, Phys. Rev. Lett. 89 (2002) 121801, arXiv:hep-ex/0204018.

[43] W.T. Eadie, et al., Statistical Methods in Experimental Physics, North Holland, Amsterdam, 1971.

[44] A.R. Bohm, Y. Sato, Relativistic resonances: their masses, widths, lifetimes, superposition, and causal evolution, Phys. Rev. D 71 (2005) 085018, arXiv:hep-ph/0412106.

[45] T.J. Humanic, Hadronic observables from Au+Au collisions at $\sqrt{s_{\rm NN}} = 200$ GeV and Pb+Pb collisions at $\sqrt{s_{\rm NN}} = 5.5$ TeV from a simple kinematic model, Phys. Rev. C 79 (2009) 044902, arXiv:0810.0621 [nucl-th].

ALICE Collaboration

S. Acharya [128], D. Adamová [87], G. Aglieri Rinella [33], L. Aglietta [25], M. Agnello [30], N. Agrawal [26], Z. Ahammed [136], S. Ahmad [16], S.U. Ahn [72], I. Ahuja [38], A. Akindinov [142], M. Al-Turany [98], D. Aleksandrov [142], B. Alessandro [57], H.M. Alfanda [6], R. Alfaro Molina [68], B. Ali [16], A. Alici [26], N. Alizadehvandchali [117], A. Alkin [33], J. Alme [21], G. Alocco [53], T. Alt [65], A.R. Altamura [51], I. Altsybeev [96], J.R. Alvarado [45], M.N. Anaam [6], C. Andrei [46], N. Andreou [116], A. Andronic [127], E. Andronov [142], V. Anguelov [95], F. Antinori [55], P. Antonioli [52], N. Apadula [75], L. Aphecetche [104], H. Appelshäuser [65], C. Arata [74], S. Arcelli [26], M. Aresti [23], R. Arnaldi [57], J.G.M.C.A. Arneiro [111], I.C. Arsene [20], M. Arslandok [139], A. Augustinus [33], R. Averbeck [98], M.D. Azmi [16], H. Baba [125], A. Badalà [54], J. Bae [105], Y.W. Baek [41], X. Bai [121], R. Bailhache [65], Y. Bailung [49], R. Bala [92], A. Balbino [30], A. Baldisseri [131], B. Balis [2], D. Banerjee [4], Z. Banoo [92], F. Barile [32], L. Barioglio [57], M. Barlou [79], B. Barman [42], G.G. Barnaföldi [47], L.S. Barnby [116], E. Barreau [104], V. Barret [128], L. Barreto [111], C. Bartels [120], K. Barth [33], E. Bartsch [65], N. Bastid [128], S. Basu [76], G. Batigne [104], D. Battistini [96], B. Batyunya [143], D. Bauri [48], J.L. Bazo Alba [102], I.G. Bearden [84], C. Beattie [139],

P. Becht [98], D. Behera [49], I. Belikov [130], A.D.C. Bell Hechavarria [127], F. Bellini [26], R. Bellwied [117], S. Belokurova [142], L.G.E. Beltran [110], Y.A.V. Beltran [45], G. Bencedi [47], A. Bensaoula [117], S. Beole [25], Y. Berdnikov [142], A. Berdnikova [95], L. Bergmann [95], M.G. Besoiu [64], L. Betev [33], P.P. Bhaduri [136], A. Bhasin [92], M.A. Bhat [4], B. Bhattacharjee [42], L. Bianchi [25], N. Bianchi [50], J. Bielčík [36], J. Bielčíková [87], A.P. Bigot [130], A. Bilandzic [96], G. Biro [47], S. Biswas [4], N. Bize [104], J.T. Blair [109], D. Blau [142], M.B. Blidaru [98], N. Bluhme [39], C. Blume [65], G. Boca [22,56], F. Bock [88], T. Bodova [21], S. Boi [23], J. Bok [17], L. Boldizsár [47], M. Bombara [38], P.M. Bond [33], G. Bonomi [135,56], H. Borel [131], A. Borissov [142], A.G. Borquez Carcamo [95], H. Bossi [139], E. Botta [25], Y.E.M. Bouziani [65], L. Bratrud [65], P. Braun-Munzinger [98], M. Bregant [111], M. Broz [36], G.E. Bruno [97,32], M.D. Buckland [24], D. Budnikov [142], H. Buesching [65], S. Bufalino [30], P. Buhler [103], N. Burmasov [142], Z. Buthelezi [69,124], A. Bylinkin [21], S.A. Bysiak [108], J.C. Cabanillas Noris [110], M.F.T. Cabrera [117], M. Cai [6], H. Caines [139], A. Caliva [29], E. Calvo Villar [102], J.M.M. Camacho [110], P. Camerini [24], F.D.M. Canedo [111], S.L. Cantway [139], M. Carabas [114], A.A. Carballo [33], F. Carnesecchi [33], R. Caron [129], L.A.D. Carvalho [111], J. Castillo Castellanos [131], F. Catalano [33,25], S. Cattaruzzi [24], C. Ceballos Sanchez [143], R. Cerri [25], I. Chakaberia [75], P. Chakraborty [137,48], S. Chandra [136], S. Chapeland [33], M. Chartier [120], S. Chattopadhyay [136], S. Chattopadhyay [100], T. Cheng [98,6], C. Cheshkov [129], V. Chibante Barroso [33], D.D. Chinellato [112], E.S. Chizzali [96,II], J. Cho [59], S. Cho [59], P. Chochula [33], D. Choudhury [42], P. Christakoglou [85], C.H. Christensen [84], P. Christiansen [76], T. Chujo [126], M. Ciacco [30], C. Cicalo [53], M.R. Ciupek [98], G. Clai [52,III], F. Colamaria [51], J.S. Colburn [101], D. Colella [97,32], M. Colocci [26], M. Concas [33], G. Conesa Balbastre [74], Z. Conesa del Valle [132], G. Contin [24], J.G. Contreras [36], M.L. Coquet [131], P. Cortese [134,57], M.R. Cosentino [113], F. Costa [33], S. Costanza [22,56], C. Cot [132], J. Crkovská [95], P. Crochet [128], R. Cruz-Torres [75], P. Cui [6], A. Dainese [55], M.C. Danisch [95], A. Danu [64], P. Das [81], P. Das [4], S. Das [4], A.R. Dash [127], S. Dash [48], A. De Caro [29], G. de Cataldo [51], J. de Cuveland [39], A. De Falco [23], D. De Gruttola [29], N. De Marco [57], C. De Martin [24], S. De Pasquale [29], R. Deb [135], R. Del Grande [96], L. Dello Stritto [33,29], W. Deng [6], P. Dhankher [19], D. Di Bari [32], A. Di Mauro [33], B. Diab [131], R.A. Diaz [143,7], T. Dietel [115], Y. Ding [6], J. Ditzel [65], R. Divià [33], D.U. Dixit [19], Ø. Djuvsland [21], U. Dmitrieva [142], A. Dobrin [64], B. Dönigus [65], J.M. Dubinski [137], A. Dubla [98], S. Dudi [91], P. Dupieux [128], M. Durkac [107], N. Dzalaiova [13], T.M. Eder [127], R.J. Ehlers [75], F. Eisenhut [65], R. Ejima [93], D. Elia [51], B. Erazmus [104], F. Ercolessi [26], B. Espagnon [132], G. Eulisse [33], D. Evans [101], S. Evdokimov [142], L. Fabbietti [96], M. Faggin [28], J. Faivre [74], F. Fan [6], W. Fan [75], A. Fantoni [50], M. Fasel [88], A. Feliciello [57], G. Feofilov [142], A. Fernández Téllez [45], L. Ferrandi [111], M.B. Ferrer [33], A. Ferrero [131], C. Ferrero [57,IV], A. Ferretti [25], V.J.G. Feuillard [95], V. Filova [36], D. Finogeev [142], F.M. Fionda [53], E. Flatland [33], F. Flor [117], A.N. Flores [109], S. Foertsch [69], I. Fokin [95], S. Fokin [142], E. Fragiacomo [58], E. Frajna [47], U. Fuchs [33], N. Funicello [29], C. Furget [74], A. Furs [142], T. Fusayasu [99], J.J. Gaardhøje [84], M. Gagliardi [25], A.M. Gago [102], T. Gahlaut [48], C.D. Galvan [110], D.R. Gangadharan [117], P. Ganoti [79], C. Garabatos [98], T. García Chávez [45], E. Garcia-Solis [9], C. Gargiulo [33], P. Gasik [98], A. Gautam [119], M.B. Gay Ducati [67], M. Germain [104], A. Ghimouz [126], C. Ghosh [136], M. Giacalone [52], G. Gioachin [30], P. Giubellino [98,57], P. Giubilato [28], A.M.C. Glaenzer [131], P. Glässel [95], E. Glimos [123], D.J.Q. Goh [77], V. Gonzalez [138], P. Gordeev [142], M. Gorgon [2], K. Goswami [49], S. Gotovac [34], V. Grabski [68], L.K. Graczykowski [137], E. Grecka [87], A. Grelli [60], C. Grigoras [33], V. Grigoriev [142], S. Grigoryan [143,1], F. Grosa [33], J.F. Grosse-Oetringhaus [33], R. Grosso [98], D. Grund [36], N.A. Grunwald [95], G.G. Guardiano [112], R. Guernane [74], M. Guilbaud [104],

K. Gulbrandsen [84], T. Gündem [65], T. Gunji [125], W. Guo [6], A. Gupta [92], R. Gupta [92], R. Gupta [49], K. Gwizdziel [137], L. Gyulai [47], C. Hadjidakis [132], F.U. Haider [92], S. Haidlova [36], M. Haldar [4], H. Hamagaki [77], A. Hamdi [75], Y. Han [140], B.G. Hanley [138], R. Hannigan [109], J. Hansen [76], J.W. Harris [139], A. Harton [9], M.V. Hartung [65], H. Hassan [118], D. Hatzifotiadou [52], P. Hauer [43], L.B. Havener [139], E. Hellbär [98], H. Helstrup [35], M. Hemmer [65], T. Herman [36], S.G. Hernandez [117], G. Herrera Corral [8], F. Herrmann [127], S. Herrmann [129], K.F. Hetland [35], B. Heybeck [65], H. Hillemanns [33], B. Hippolyte [130], F.W. Hoffmann [71], B. Hofman [60], G.H. Hong [140], M. Horst [96], A. Horzyk [2], Y. Hou [6], P. Hristov [33], P. Huhn [65], L.M. Huhta [118], T.J. Humanic [89], A. Hutson [117], D. Hutter [39], M.C. Hwang [19], R. Ilkaev [142], H. Ilyas [14], M. Inaba [126], G.M. Innocenti [33], M. Ippolitov [142], A. Isakov [85], T. Isidori [119], M.S. Islam [100], M. Ivanov [98], M. Ivanov [13], V. Ivanov [142], K.E. Iversen [76], M. Jablonski [2], B. Jacak [19,75], N. Jacazio [26], P.M. Jacobs [75], S. Jadlovska [107], J. Jadlovsky [107], S. Jaelani [83], C. Jahnke [111], M.J. Jakubowska [137], M.A. Janik [137], T. Janson [71], S. Ji [17], S. Jia [10], A.A.P. Jimenez [66], F. Jonas [75,88,127], D.M. Jones [120], J.M. Jowett [33,98], J. Jung [65], M. Jung [65], A. Junique [33], A. Jusko [101], J. Kaewjai [106], P. Kalinak [61], A.S. Kalteyer [98], A. Kalweit [33], A. Karasu Uysal [73,V], D. Karatovic [90], O. Karavichev [142], T. Karavicheva [142], P. Karczmarczyk [137], E. Karpechev [142], M.J. Karwowska [33,137], U. Kebschull [71], R. Keidel [141], D.L.D. Keijdener [60], M. Keil [33], B. Ketzer [43], S.S. Khade [49], A.M. Khan [121], S. Khan [16], A. Khanzadeev [142], Y. Kharlov [142], A. Khatun [119], A. Khuntia [36], Z. Khuranova [65], B. Kileng [35], B. Kim [105], C. Kim [17], D.J. Kim [118], E.J. Kim [70], J. Kim [140], J. Kim [59], J. Kim [70], M. Kim [19], S. Kim [18], T. Kim [140], K. Kimura [93], A. Kirkova [37], S. Kirsch [65], I. Kisel [39], S. Kiselev [142], A. Kisiel [137], J.P. Kitowski [2], J.L. Klay [5], J. Klein [33], S. Klein [75], C. Klein-Bösing [127], M. Kleiner [65], T. Klemenz [96], A. Kluge [33], C. Kobdaj [106], T. Kollegger [98], A. Kondratyev [143], N. Kondratyeva [142], J. Konig [65], S.A. Konigstorfer [96], P.J. Konopka [33], G. Kornakov [137], M. Korwieser [96], S.D. Koryciak [2], A. Kotliarov [87], N. Kovacic [90], V. Kovalenko [142], M. Kowalski [108], V. Kozhuharov [37], I. Králik [61], A. Kravčáková [38], L. Krcal [33,39], M. Krivda [101,61], F. Krizek [87], K. Krizkova Gajdosova [33], M. Kroesen [95], M. Krüger [65], D.M. Krupova [36], E. Kryshen [142], V. Kučera [59], C. Kuhn [130], P.G. Kuijer [85], T. Kumaoka [126], D. Kumar [136], L. Kumar [91], N. Kumar [91], S. Kumar [32], S. Kundu [33], P. Kurashvili [80], A. Kurepin [142], A.B. Kurepin [142], A. Kuryakin [142], S. Kushpil [87], V. Kuskov [142], M. Kutyla [137], M.J. Kweon [59], Y. Kwon [140], S.L. La Pointe [39], P. La Rocca [27], A. Lakrathok [106], M. Lamanna [33], A.R. Landou [74], R. Langoy [122], P. Larionov [33], E. Laudi [33], L. Lautner [33,96], R. Lavicka [103], R. Lea [135,56], H. Lee [105], I. Legrand [46], G. Legras [127], J. Lehrbach [39], T.M. Lelek [2], R.C. Lemmon [86], I. León Monzón [110], M.M. Lesch [96], E.D. Lesser [19], P. Lévai [47], X. Li [10], B.E. Liang-gilman [19], J. Lien [122], R. Lietava [101], I. Likmeta [117], B. Lim [25], S.H. Lim [17], V. Lindenstruth [39], A. Lindner [46], C. Lippmann [98], D.H. Liu [6], J. Liu [120], G.S.S. Liveraro [112], I.M. Lofnes [21], C. Loizides [88], S. Lokos [108], J. Lömker [60], P. Loncar [34], X. Lopez [128], E. López Torres [7], P. Lu [98,121], F.V. Lugo [68], J.R. Luhder [127], M. Lunardon [28], G. Luparello [58], Y.G. Ma [40], M. Mager [33], A. Maire [130], E.M. Majerz [2], M.V. Makariev [37], M. Malaev [142], G. Malfattore [26], N.M. Malik [92], Q.W. Malik [20], S.K. Malik [92], L. Malinina [143,I,VIII], D. Mallick [132], N. Mallick [49], G. Mandaglio [31,54], S.K. Mandal [80], V. Manko [142], F. Manso [128], V. Manzari [51], Y. Mao [6], R.W. Marcjan [2], G.V. Margagliotti [24], A. Margotti [52], A. Marín [98], C. Markert [109], P. Martinengo [33], M.I. Martínez [45], G. Martínez García [104], M.P.P. Martins [111], S. Masciocchi [98], M. Masera [25], A. Masoni [53], L. Massacrier [132], O. Massen [60], A. Mastroserio [133,51], O. Matonoha [76], S. Mattiazzo [28], A. Matyja [108], C. Mayer [108],

A.L. Mazuecos [33], F. Mazzaschi [25], M. Mazzilli [33], J.E. Mdhluli [124], Y. Melikyan [44], A. Menchaca-Rocha [68], J.E.M. Mendez [66], E. Meninno [103], A.S. Menon [117], M. Meres [13], Y. Miake [126], L. Micheletti [33], D.L. Mihaylov [96], K. Mikhaylov [143,142], D. Miśkowiec [98], A. Modak [4], B. Mohanty [81], M. Mohisin Khan [16,VI], M.A. Molander [44], S. Monira [137], C. Mordasini [118], D.A. Moreira De Godoy [127], I. Morozov [142], A. Morsch [33], T. Mrnjavac [33], V. Muccifora [50], S. Muhuri [136], J.D. Mulligan [75], A. Mulliri [23], M.G. Munhoz [111], R.H. Munzer [65], H. Murakami [125], S. Murray [115], L. Musa [33], J. Musinsky [61], J.W. Myrcha [137], B. Naik [124], A.I. Nambrath [19], B.K. Nandi [48], R. Nania [52], E. Nappi [51], A.F. Nassirpour [18], A. Nath [95], C. Nattrass [123], M.N. Naydenov [37], A. Neagu [20], A. Negru [114], E. Nekrasova [142], L. Nellen [66], R. Nepeivoda [76], S. Nese [20], G. Neskovic [39], N. Nicassio [51], B.S. Nielsen [84], E.G. Nielsen [84], S. Nikolaev [142], S. Nikulin [142], V. Nikulin [142], F. Noferini [52], S. Noh [12], P. Nomokonov [143], J. Norman [120], N. Novitzky [88], P. Nowakowski [137], A. Nyanin [142], J. Nystrand [21], S. Oh [18], A. Ohlson [76], V.A. Okorokov [142], J. Oleniacz [137], A. Onnerstad [118], C. Oppedisano [57], A. Ortiz Velasquez [66], J. Otwinowski [108], M. Oya [93], K. Oyama [77], Y. Pachmayer [95], S. Padhan [48], D. Pagano [135,56], G. Paić [66], S. Paisano-Guzmán [45], A. Palasciano [51], S. Panebianco [131], H. Park [126], H. Park [105], J. Park [59], J.E. Parkkila [33], Y. Patley [48], B. Paul [23], M.M.D.M. Paulino [111], H. Pei [6], T. Peitzmann [60], X. Peng [11], M. Pennisi [25], S. Perciballi [25], D. Peresunko [142], G.M. Perez [7], Y. Pestov [142], V. Petrov [142], M. Petrovici [46], R.P. Pezzi [104,67], S. Piano [58], M. Pikna [13], P. Pillot [104], O. Pinazza [52,33], L. Pinsky [117], C. Pinto [96], S. Pisano [50], M. Płoskoń [75], M. Planinic [90], F. Pliquett [65], M.G. Poghosyan [88], B. Polichtchouk [142], S. Politano [30], N. Poljak [90], A. Pop [46], S. Porteboeuf-Houssais [128], V. Pozdniakov [143], I.Y. Pozos [45], K.K. Pradhan [49], S.K. Prasad [4], S. Prasad [49], R. Preghenella [52], F. Prino [57], C.A. Pruneau [138], I. Pshenichnov [142], M. Puccio [33], S. Pucillo [25], Z. Pugelova [107], S. Qiu [85], L. Quaglia [25], S. Ragoni [15], A. Rai [139], A. Rakotozafindrabe [131], L. Ramello [134,57], F. Rami [130], M. Rasa [27], S.S. Räsänen [44], R. Rath [52], M.P. Rauch [21], I. Ravasenga [33], K.F. Read [88,123], C. Reckziegel [113], A.R. Redelbach [39], K. Redlich [80,VII], C.A. Reetz [98], H.D. Regules-Medel [45], A. Rehman [21], F. Reidt [33], H.A. Reme-Ness [35], Z. Rescakova [38], K. Reygers [95], A. Riabov [142], V. Riabov [142], R. Ricci [29], M. Richter [20], A.A. Riedel [96], W. Riegler [33], A.G. Riffero [25], C. Ristea [64], M.V. Rodriguez [33], M. Rodríguez Cahuantzi [45], S.A. Rodríguez Ramírez [45], K. Røed [20], R. Rogalev [142], E. Rogochaya [143], T.S. Rogoschinski [65], D. Rohr [33], D. Röhrich [21], P.F. Rojas [45], S. Rojas Torres [36], P.S. Rokita [137], G. Romanenko [26], F. Ronchetti [50], A. Rosano [31,54], E.D. Rosas [66], K. Roslon [137], A. Rossi [55], A. Roy [49], S. Roy [48], N. Rubini [26], D. Ruggiano [137], R. Rui [24], P.G. Russek [2], R. Russo [85], A. Rustamov [82], E. Ryabinkin [142], Y. Ryabov [142], A. Rybicki [108], H. Rytkonen [118], J. Ryu [17], W. Rzesa [137], O.A.M. Saarimaki [44], S. Sadhu [32], S. Sadovsky [142], J. Saetre [21], K. Šafařík [36], S.K. Saha [4], S. Saha [81], B. Sahoo [49], R. Sahoo [49], S. Sahoo [62], D. Sahu [49], P.K. Sahu [62], J. Saini [136], K. Sajdakova [38], S. Sakai [126], M.P. Salvan [98], S. Sambyal [92], D. Samitz [103], I. Sanna [33,96], T.B. Saramela [111], D. Sarkar [84], P. Sarma [42], V. Sarritzu [23], V.M. Sarti [96], M.H.P. Sas [33], S. Sawan [81], E. Scapparone [52], J. Schambach [88], H.S. Scheid [65], C. Schiaua [46], R. Schicker [95], F. Schlepper [95], A. Schmah [98], C. Schmidt [98], H.R. Schmidt [94], M.O. Schmidt [33], M. Schmidt [94], N.V. Schmidt [88], A.R. Schmier [123], R. Schotter [130], A. Schröter [39], J. Schukraft [33], K. Schweda [98], G. Scioli [26], E. Scomparin [57], J.E. Seger [15], Y. Sekiguchi [125], D. Sekihata [125], M. Selina [85], I. Selyuzhenkov [98], S. Senyukov [130], J.J. Seo [95], D. Serebryakov [142], L. Serkin [66], L. Šerkšnytė [96], A. Sevcenco [64], T.J. Shaba [69], A. Shabetai [104], R. Shahoyan [33], A. Shangaraev [142], B. Sharma [92], D. Sharma [48],

H. Sharma [55], M. Sharma [92], S. Sharma [77], S. Sharma [92], U. Sharma [92], A. Shatat [132], O. Sheibani [117], K. Shigaki [93], M. Shimomura [78], J. Shin [12], S. Shirinkin [142], Q. Shou [40], Y. Sibiriak [142], S. Siddhanta [53], T. Siemiarczuk [80], T.F. Silva [111], D. Silvermyr [76], T. Simantathammakul [106], R. Simeonov [37], B. Singh [92], B. Singh [96], K. Singh [49], R. Singh [81], R. Singh [92], R. Singh [98,49], S. Singh [16], V.K. Singh [136], V. Singhal [136], T. Sinha [100], B. Sitar [13], M. Sitta [134,57], T.B. Skaali [20], G. Skorodumovs [95], M. Slupecki [44], N. Smirnov [139], R.J.M. Snellings [60], E.H. Solheim [20], J. Song [17], C. Sonnabend [33,98], J.M. Sonneveld [85], F. Soramel [28], A.B. Soto-hernandez [89], R. Spijkers [85], I. Sputowska [108], J. Staa [76], J. Stachel [95], I. Stan [64], P.J. Steffanic [123], S.F. Stiefelmaier [95], D. Stocco [104], I. Storehaug [20], P. Stratmann [127], S. Strazzi [26], A. Sturniolo [31,54], C.P. Stylianidis [85], A.A.P. Suaide [111], C. Suire [132], M. Sukhanov [142], M. Suljic [33], R. Sultanov [142], V. Sumberia [92], S. Sumowidagdo [83], I. Szarka [13], M. Szymkowski [137], S.F. Taghavi [96], G. Taillepied [98], J. Takahashi [112], G.J. Tambave [81], S. Tang [6], Z. Tang [121], J.D. Tapia Takaki [119], N. Tapus [114], L.A. Tarasovicova [127], M.G. Tarzila [46], G.F. Tassielli [32], A. Tauro [33], A. Tavira García [132], G. Tejeda Muñoz [45], A. Telesca [33], L. Terlizzi [25], C. Terrevoli [117], S. Thakur [4], D. Thomas [109], A. Tikhonov [142], N. Tiltmann [33,127], A.R. Timmins [117], M. Tkacik [107], T. Tkacik [107], A. Toia [65], R. Tokumoto [93], K. Tomohiro [93], N. Topilskaya [142], M. Toppi [50], T. Tork [132], V.V. Torres [104], A.G. Torres Ramos [32], A. Trifiró [31,54], A.S. Triolo [33,31,54], S. Tripathy [52], T. Tripathy [48], S. Trogolo [33], V. Trubnikov [3], W.H. Trzaska [118], T.P. Trzcinski [137], A. Tumkin [142], R. Turrisi [55], T.S. Tveter [20], K. Ullaland [21], B. Ulukutlu [96], A. Uras [129], M. Urioni [135], G.L. Usai [23], M. Vala [38], N. Valle [22], L.V.R. van Doremalen [60], M. van Leeuwen [85], C.A. van Veen [95], R.J.G. van Weelden [85], P. Vande Vyvre [33], D. Varga [47], Z. Varga [47], P. Vargas Torres [66], M. Vasileiou [79], A. Vasiliev [142], O. Vázquez Doce [50], O. Vazquez Rueda [117], V. Vechernin [142], E. Vercellin [25], S. Vergara Limón [45], R. Verma [48], L. Vermunt [98], R. Vértesi [47], M. Verweij [60], L. Vickovic [34], Z. Vilakazi [124], O. Villalobos Baillie [101], A. Villani [24], A. Vinogradov [142], T. Virgili [29], M.M.O. Virta [118], V. Vislavicius [76], A. Vodopyanov [143], B. Volkel [33], M.A. Völkl [95], S.A. Voloshin [138], G. Volpe [32], B. von Haller [33], I. Vorobyev [33], N. Vozniuk [142], J. Vrláková [38], J. Wan [40], C. Wang [40], D. Wang [40], Y. Wang [40], Y. Wang [6], A. Wegrzynek [33], F.T. Weiglhofer [39], S.C. Wenzel [33], J.P. Wessels [127], J. Wiechula [65], J. Wikne [20], G. Wilk [80], J. Wilkinson [98], G.A. Willems [127], B. Windelband [95], M. Winn [131], J.R. Wright [109], W. Wu [40], Y. Wu [121], Z. Xiong [121], R. Xu [6], A. Yadav [43], A.K. Yadav [136], S. Yalcin [73], Y. Yamaguchi [93], S. Yang [21], S. Yano [93], E.R. Yeats [19], Z. Yin [6], I.-K. Yoo [17], J.H. Yoon [59], H. Yu [12], S. Yuan [21], A. Yuncu [95], V. Zaccolo [24], C. Zampolli [33], F. Zanone [95], N. Zardoshti [33], A. Zarochentsev [142], P. Závada [63], N. Zaviyalov [142], M. Zhalov [142], B. Zhang [6], C. Zhang [131], L. Zhang [40], M. Zhang [6], S. Zhang [40], X. Zhang [6], Y. Zhang [121], Z. Zhang [6], M. Zhao [10], V. Zherebchevskii [142], Y. Zhi [10], C. Zhong [40], D. Zhou [6], Y. Zhou [84], J. Zhu [55,6], Y. Zhu [6], S.C. Zugravel [57], N. Zurlo [135,56]

[1] A.I. Alikhanyan National Science Laboratory (Yerevan Physics Institute) Foundation, Yerevan, Armenia
[2] AGH University of Krakow, Cracow, Poland
[3] Bogolyubov Institute for Theoretical Physics, National Academy of Sciences of Ukraine, Kiev, Ukraine
[4] Bose Institute, Department of Physics and Centre for Astroparticle Physics and Space Science (CAPSS), Kolkata, India
[5] California Polytechnic State University, San Luis Obispo, CA, United States
[6] Central China Normal University, Wuhan, China
[7] Centro de Aplicaciones Tecnológicas y Desarrollo Nuclear (CEADEN), Havana, Cuba
[8] Centro de Investigación y de Estudios Avanzados (CINVESTAV), Mexico City and Mérida, Mexico
[9] Chicago State University, Chicago, IL, United States
[10] China Institute of Atomic Energy, Beijing, China
[11] China University of Geosciences, Wuhan, China
[12] Chungbuk National University, Cheongju, Republic of Korea
[13] Comenius University Bratislava, Faculty of Mathematics, Physics and Informatics, Bratislava, Slovak Republic
[14] COMSATS University Islamabad, Islamabad, Pakistan
[15] Creighton University, Omaha, NE, United States

[16] Department of Physics, Aligarh Muslim University, Aligarh, India
[17] Department of Physics, Pusan National University, Pusan, Republic of Korea
[18] Department of Physics, Sejong University, Seoul, Republic of Korea
[19] Department of Physics, University of California, Berkeley, CA, United States
[20] Department of Physics, University of Oslo, Oslo, Norway
[21] Department of Physics and Technology, University of Bergen, Bergen, Norway
[22] Dipartimento di Fisica, Università di Pavia, Pavia, Italy
[23] Dipartimento di Fisica dell'Università and Sezione INFN, Cagliari, Italy
[24] Dipartimento di Fisica dell'Università and Sezione INFN, Trieste, Italy
[25] Dipartimento di Fisica dell'Università and Sezione INFN, Turin, Italy
[26] Dipartimento di Fisica e Astronomia dell'Università and Sezione INFN, Bologna, Italy
[27] Dipartimento di Fisica e Astronomia dell'Università and Sezione INFN, Catania, Italy
[28] Dipartimento di Fisica e Astronomia dell'Università and Sezione INFN, Padova, Italy
[29] Dipartimento di Fisica 'E.R. Caianiello' dell'Università and Gruppo Collegato INFN, Salerno, Italy
[30] Dipartimento DISAT del Politecnico and Sezione INFN, Turin, Italy
[31] Dipartimento di Scienze MIFT, Università di Messina, Messina, Italy
[32] Dipartimento Interateneo di Fisica 'M. Merlin' and Sezione INFN, Bari, Italy
[33] European Organization for Nuclear Research (CERN), Geneva, Switzerland
[34] Faculty of Electrical Engineering, Mechanical Engineering and Naval Architecture, University of Split, Split, Croatia
[35] Faculty of Engineering and Science, Western Norway University of Applied Sciences, Bergen, Norway
[36] Faculty of Nuclear Sciences and Physical Engineering, Czech Technical University in Prague, Prague, Czech Republic
[37] Faculty of Physics, Sofia University, Sofia, Bulgaria
[38] Faculty of Science, P.J. Šafárik University, Košice, Slovak Republic
[39] Frankfurt Institute for Advanced Studies, Johann Wolfgang Goethe-Universität Frankfurt, Frankfurt, Germany
[40] Fudan University, Shanghai, China
[41] Gangneung-Wonju National University, Gangneung, Republic of Korea
[42] Gauhati University, Department of Physics, Guwahati, India
[43] Helmholtz-Institut für Strahlen- und Kernphysik, Rheinische Friedrich-Wilhelms-Universität Bonn, Bonn, Germany
[44] Helsinki Institute of Physics (HIP), Helsinki, Finland
[45] High Energy Physics Group, Universidad Autónoma de Puebla, Puebla, Mexico
[46] Horia Hulubei National Institute of Physics and Nuclear Engineering, Bucharest, Romania
[47] HUN-REN Wigner Research Centre for Physics, Budapest, Hungary
[48] Indian Institute of Technology Bombay (IIT), Mumbai, India
[49] Indian Institute of Technology Indore, Indore, India
[50] INFN, Laboratori Nazionali di Frascati, Frascati, Italy
[51] INFN, Sezione di Bari, Bari, Italy
[52] INFN, Sezione di Bologna, Bologna, Italy
[53] INFN, Sezione di Cagliari, Cagliari, Italy
[54] INFN, Sezione di Catania, Catania, Italy
[55] INFN, Sezione di Padova, Padova, Italy
[56] INFN, Sezione di Pavia, Pavia, Italy
[57] INFN, Sezione di Torino, Turin, Italy
[58] INFN, Sezione di Trieste, Trieste, Italy
[59] Inha University, Incheon, Republic of Korea
[60] Institute for Gravitational and Subatomic Physics (GRASP), Utrecht University/Nikhef, Utrecht, Netherlands
[61] Institute of Experimental Physics, Slovak Academy of Sciences, Košice, Slovak Republic
[62] Institute of Physics, Homi Bhabha National Institute, Bhubaneswar, India
[63] Institute of Physics of the Czech Academy of Sciences, Prague, Czech Republic
[64] Institute of Space Science (ISS), Bucharest, Romania
[65] Institut für Kernphysik, Johann Wolfgang Goethe-Universität Frankfurt, Frankfurt, Germany
[66] Instituto de Ciencias Nucleares, Universidad Nacional Autónoma de México, Mexico City, Mexico
[67] Instituto de Física, Universidade Federal do Rio Grande do Sul (UFRGS), Porto Alegre, Brazil
[68] Instituto de Física, Universidad Nacional Autónoma de México, Mexico City, Mexico
[69] iThemba LABS, National Research Foundation, Somerset West, South Africa
[70] Jeonbuk National University, Jeonju, Republic of Korea
[71] Johann-Wolfgang-Goethe Universität Frankfurt Institut für Informatik, Fachbereich Informatik und Mathematik, Frankfurt, Germany
[72] Korea Institute of Science and Technology Information, Daejeon, Republic of Korea
[73] KTO Karatay University, Konya, Turkey
[74] Laboratoire de Physique Subatomique et de Cosmologie, Université Grenoble-Alpes, CNRS-IN2P3, Grenoble, France
[75] Lawrence Berkeley National Laboratory, Berkeley, CA, United States
[76] Lund University Department of Physics, Division of Particle Physics, Lund, Sweden
[77] Nagasaki Institute of Applied Science, Nagasaki, Japan
[78] Nara Women's University (NWU), Nara, Japan
[79] National and Kapodistrian University of Athens, School of Science, Department of Physics, Athens, Greece
[80] National Centre for Nuclear Research, Warsaw, Poland
[81] National Institute of Science Education and Research, Homi Bhabha National Institute, Jatni, India
[82] National Nuclear Research Center, Baku, Azerbaijan
[83] National Research and Innovation Agency – BRIN, Jakarta, Indonesia
[84] Niels Bohr Institute, University of Copenhagen, Copenhagen, Denmark
[85] Nikhef, National institute for subatomic physics, Amsterdam, Netherlands
[86] Nuclear Physics Group, STFC Daresbury Laboratory, Daresbury, United Kingdom
[87] Nuclear Physics Institute of the Czech Academy of Sciences, Husinec-Řež, Czech Republic
[88] Oak Ridge National Laboratory, Oak Ridge, TN, United States
[89] Ohio State University, Columbus, OH, United States
[90] Physics department, Faculty of science, University of Zagreb, Zagreb, Croatia
[91] Physics Department, Panjab University, Chandigarh, India
[92] Physics Department, University of Jammu, Jammu, India
[93] Physics Program and International Institute for Sustainability with Knotted Chiral Meta Matter (SKCM2), Hiroshima University, Hiroshima, Japan
[94] Physikalisches Institut, Eberhard-Karls-Universität Tübingen, Tübingen, Germany
[95] Physikalisches Institut, Ruprecht-Karls-Universität Heidelberg, Heidelberg, Germany

[96] Physik Department, Technische Universität München, Munich, Germany
[97] Politecnico di Bari and Sezione INFN, Bari, Italy
[98] Research Division and ExtreMe Matter Institute EMMI, GSI Helmholtzzentrum für Schwerionenforschung GmbH, Darmstadt, Germany
[99] Saga University, Saga, Japan
[100] Saha Institute of Nuclear Physics, Homi Bhabha National Institute, Kolkata, India
[101] School of Physics and Astronomy, University of Birmingham, Birmingham, United Kingdom
[102] Sección Física, Departamento de Ciencias, Pontificia Universidad Católica del Perú, Lima, Peru
[103] Stefan Meyer Institut für Subatomare Physik (SMI), Vienna, Austria
[104] SUBATECH, IMT Atlantique, Nantes Université, CNRS-IN2P3, Nantes, France
[105] Sungkyunkwan University, Suwon City, Republic of Korea
[106] Suranaree University of Technology, Nakhon Ratchasima, Thailand
[107] Technical University of Košice, Košice, Slovak Republic
[108] The Henryk Niewodniczanski Institute of Nuclear Physics, Polish Academy of Sciences, Cracow, Poland
[109] The University of Texas at Austin, Austin, TX, United States
[110] Universidad Autónoma de Sinaloa, Culiacán, Mexico
[111] Universidade de São Paulo (USP), São Paulo, Brazil
[112] Universidade Estadual de Campinas (UNICAMP), Campinas, Brazil
[113] Universidade Federal do ABC, Santo Andre, Brazil
[114] Universitatea Nationala de Stiinta si Tehnologie Politehnica Bucuresti, Bucharest, Romania
[115] University of Cape Town, Cape Town, South Africa
[116] University of Derby, Derby, United Kingdom
[117] University of Houston, Houston, TX, United States
[118] University of Jyväskylä, Jyväskylä, Finland
[119] University of Kansas, Lawrence, KS, United States
[120] University of Liverpool, Liverpool, United Kingdom
[121] University of Science and Technology of China, Hefei, China
[122] University of South-Eastern Norway, Kongsberg, Norway
[123] University of Tennessee, Knoxville, TN, United States
[124] University of the Witwatersrand, Johannesburg, South Africa
[125] University of Tokyo, Tokyo, Japan
[126] University of Tsukuba, Tsukuba, Japan
[127] Universität Münster, Institut für Kernphysik, Münster, Germany
[128] Université Clermont Auvergne, CNRS/IN2P3, LPC, Clermont-Ferrand, France
[129] Université de Lyon, CNRS/IN2P3, Institut de Physique des 2 Infinis de Lyon, Lyon, France
[130] Université de Strasbourg, CNRS, IPHC UMR 7178, F-67000 Strasbourg, France
[131] Université Paris-Saclay, Centre d'Etudes de Saclay (CEA), IRFU, Départment de Physique Nucléaire (DPhN), Saclay, France
[132] Université Paris-Saclay, CNRS/IN2P3, IJCLab, Orsay, France
[133] Università degli Studi di Foggia, Foggia, Italy
[134] Università del Piemonte Orientale, Vercelli, Italy
[135] Università di Brescia, Brescia, Italy
[136] Variable Energy Cyclotron Centre, Homi Bhabha National Institute, Kolkata, India
[137] Warsaw University of Technology, Warsaw, Poland
[138] Wayne State University, Detroit, MI, United States
[139] Yale University, New Haven, CT, United States
[140] Yonsei University, Seoul, Republic of Korea
[141] Zentrum für Technologie und Transfer (ZTT), Worms, Germany
[142] Affiliated with an institute covered by a cooperation agreement with CERN
[143] Affiliated with an international laboratory covered by a cooperation agreement with CERN

[I] Deceased.
[II] Also at: Max-Planck-Institut fur Physik, Munich, Germany.
[III] Also at: Italian National Agency for New Technologies, Energy and Sustainable Economic Development (ENEA), Bologna, Italy.
[IV] Also at: Dipartimento DET del Politecnico di Torino, Turin, Italy.
[V] Also at: Yildiz Technical University, Istanbul, Türkiye.
[VI] Also at: Department of Applied Physics, Aligarh Muslim University, Aligarh, India.
[VII] Also at: Institute of Theoretical Physics, University of Wroclaw, Poland.
[VIII] Also at: An institution covered by a cooperation agreement with CERN.